

AD-A037 380

BALLISTIC RESEARCH LABS ABERDEEN PROVING GROUND MD
WIND TUNNEL TESTS OF SUPERSONIC LIFTING BODIES AT MACH NUMBER 1--ETC(U)
FEB 77 C J NIETUBICZ
BRL-MR-2728

F/G 1/3

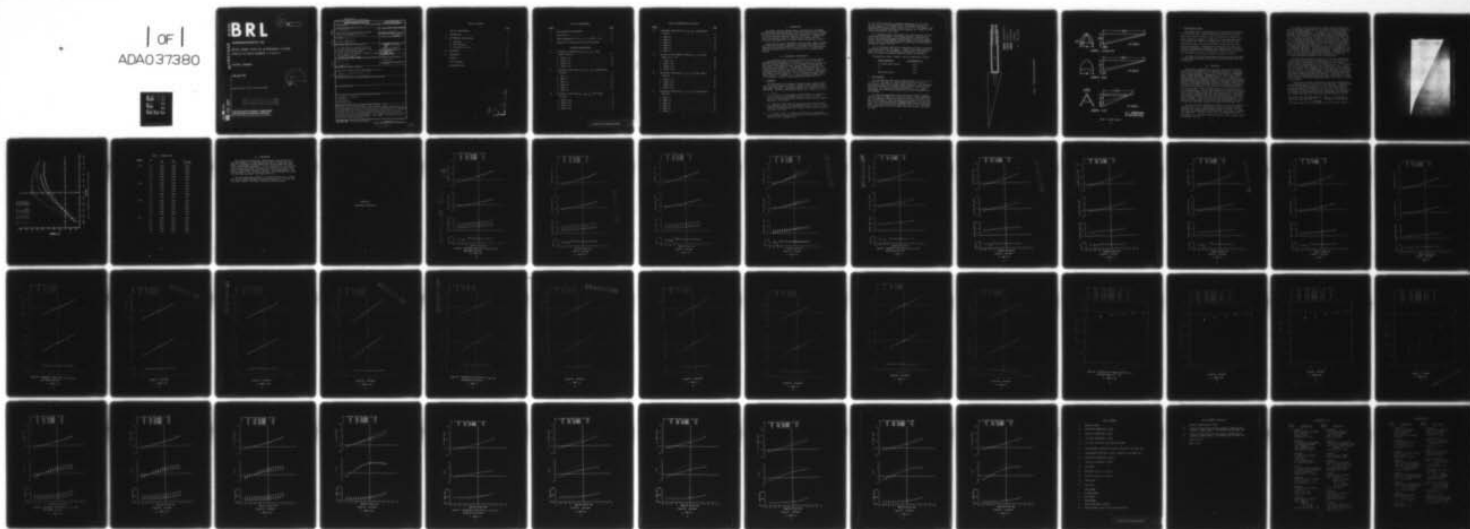
UNCLASSIFIED

NL

1 of 1
ADAO37380

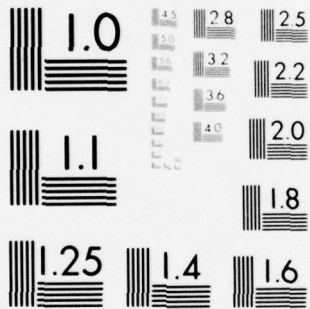


BRL



END

DATE
FILMED
4-77



MICROCOPY RESOLUTION TEST CHART
NATIONAL BUREAU OF STANDARDS-1963-A

BRL MR 2728

BRL

(12)
B5

AD

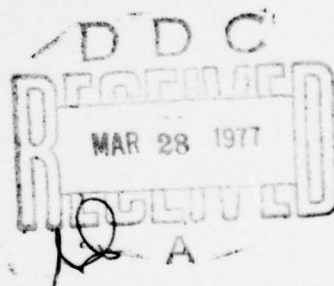
AD A 037380

MEMORANDUM REPORT NO. 2728

WIND TUNNEL TESTS OF SUPERSONIC LIFTING
BODIES AT MACH NUMBER 1.5 TO 4.0

Charles J. Nietubicz

February 1977



Approved for public release; distribution unlimited.

COPY AVAILABLE TO DDC DOES NOT
PERMIT FULLY LEGIBLE PRODUCTION

USA BALLISTIC RESEARCH LABORATORY
ABERDEEN PROVING GROUND, MARYLAND

DDC FILE COPY
NO.

UNCLASSIFIED

SECURITY CLASSIFICATION OF THIS PAGE (When Data Entered)

REPORT DOCUMENTATION PAGE		READ INSTRUCTIONS BEFORE COMPLETING FORM
1. REPORT NUMBER BRL Memorandum Report No. 2728	2. GOVT ACCESSION NO.	3. RECIPIENT'S CATALOG NUMBER
4. TITLE (and Subtitle) WIND TUNNEL TESTS OF SUPERSONIC LIFTING BODIES AT MACH NUMBER 1.5 TO 4.0	5. TYPE OF REPORT & PERIOD COVERED Final Rept.	6. PERFORMING ORG. REPORT NUMBER
7. AUTHOR(s) Charles J. Nietubicz	8. CONTRACT OR GRANT NUMBER(s)	
9. PERFORMING ORGANIZATION NAME AND ADDRESS U.S. Army Ballistic Research Laboratory Aberdeen Proving Ground, Maryland 21005	10. PROGRAM ELEMENT, PROJECT, TASK AREA & WORK UNIT NUMBERS RDT&E 1T662618AH80	
11. CONTROLLING OFFICE NAME AND ADDRESS US Army Materiel Development & Readiness Command 5001 Eisenhower Avenue Alexandria, Virginia 22333	12. REPORT DATE FEBRUARY 1977	13. NUMBER OF PAGES 57
14. MONITORING AGENCY NAME & ADDRESS (if different from Controlling Office) 52p.	15. SECURITY CLASS. (of this report) UNCLASSIFIED	15a. DECLASSIFICATION/DOWNGRADING SCHEDULE
16. DISTRIBUTION STATEMENT (of this Report) Approved for public release; distribution unlimited.		
17. DISTRIBUTION STATEMENT (of the abstract entered in Block 20, if different from Report) BRL-MR-2728		
18. SUPPLEMENTARY NOTES		
19. KEY WORDS (Continue on reverse side if necessary and identify by block number) Aerodynamic Coefficients Wave Rider Lifting Bodies Wind Tunnel Data		
20. ABSTRACT (Continue on reverse side if necessary and identify by block number) (1cb) Wind tunnel tests were conducted on four new wedge shaped configurations, one of which approached that of a wave rider design. Aerodynamic data are presented for Mach numbers 1.5 through 4.0 with angle of attack variation from -10° to $+7^\circ$. The data are similar to previously reported results with the one exception being the near wave rider configuration. This configuration resulted in lift/drag data being invariant with respect to Mach number. The maximum value of lift/drag reached approximately 3.0.		

DD FORM 1 JAN 73 1473

EDITION OF 1 NOV 65 IS OBSOLETE

UNCLASSIFIED

SECURITY CLASSIFICATION OF THIS PAGE (When Data Entered)

050750

y/b

TABLE OF CONTENTS

	<u>Page</u>
LIST OF ILLUSTRATIONS	5
I. INTRODUCTION	7
II. EXPERIMENTAL INVESTIGATION	7
A. Equipment	7
B. Test Procedure	8
C. Presentation of Data	11
III. DISCUSSION	11
IV. CONCLUSIONS	16
APPENDIX	17
LIST OF SYMBOLS	53
DISTRIBUTION LIST	55

[illegible]

LIST OF ILLUSTRATIONS

<u>Figure</u>		<u>Page</u>
1.	Model-Balance-Strut Assembly	9
2.	Model Details	10
3.	Spark Shadowgraph, $M = 3.0$, $\alpha = 0^\circ$, CONFIG = 4.00	13
4.	Comparison of Lift/Drag Data for Lifting Bodies	14

APPENDIX ILLUSTRATIONS

A1.	Aerodynamic Coefficients C_N , C_M , C_A , X_{CP} --Mach Number Variation	18
	a. CONFIG 1.00	18
	b. CONFIG 2.00	19
	c. CONFIG 3.00	20
	d. CONFIG 4.00	21
A2.	Aerodynamic Coefficients C_N , C_M , C_A , X_{CP} --Configuration Variation	22
	a. MACH 1.5	22
	b. MACH 2.0	23
	c. MACH 2.5	24
	d. MACH 3.0	25
	e. MACH 3.5	26
	f. MACH 4.0	27
A3.	Aerodynamic Coefficients C_Y , C_{YM} , Y_{CP} --Mach Number Variation	28
	a. CONFIG 1.00.	28
	b. CONFIG 2.00.	29
	c. CONFIG 3.00.	30
	d. CONFIG 4.00.	31

LIST OF ILLUSTRATIONS (Continued)

<u>Figure</u>		<u>Page</u>
A4.	Aerodynamic Coefficients C_Y , C_{YM} , Y_{CP} --Configuration Variation	32
	a. MACH 1.5	32
	b. MACH 2.0	33
	c. MACH 2.5	34
	d. MACH 3.0	35
	e. MACH 3.5	36
	f. MACH 4.0	37
A5.	Variation of Roll Moment Coefficient, C_{ℓ} , With Mach Number for $\phi = 45^\circ$	38
	a. CONFIG 1.00	38
	b. CONFIG 2.00	39
	c. CONFIG 3.00	40
	d. CONFIG 4.00	41
A6.	Aerodynamic Coefficients C_L , C_D , C_L/C_D --Mach Number Variation	42
	a. CONFIG 1.00	42
	b. CONFIG 2.00	43
	c. CONFIG 3.00	44
	d. CONFIG 4.00	45
A7.	Aerodynamic Coefficients C_L , C_D , C_L/C_D --Configuration Variation	46
	a. MACH 1.5	46
	b. MACH 2.0	47
	c. MACH 2.5	48
	d. MACH 3.0	49
	e. MACH 3.5	50
	f. MACH 4.0	51

I. INTRODUCTION

The Weapons Systems Concepts Office, Directorate of Development and Engineering, APG-Edgewood Area, under the direction of Mr. Abraham Flatau, has initiated an investigation of aeroballistic shapes designed to achieve increased range and flattened trajectories. Conceptually, this is obtained by design of a model with low overall drag and sufficient aerodynamic lift to slightly offset the affects of gravity.

Results of an initial experimental study of wedge shaped configurations have been previously reported¹. The present wind tunnel tests, conducted by the Launch and Flight Division (LFD), U.S. Army Ballistic Research Laboratory (BRL), are a continuation of the Edgewood Wedge Program.

II. EXPERIMENTAL INVESTIGATION

A six component force test was conducted for four wedge shaped configurations in Supersonic Wind Tunnel No. 1² of the U.S. Army Ballistic Research Laboratory. Three configurations were designed and fabricated by the Weapons Systems Concepts Office, Directorate of Development and Engineering. The remaining configuration was a BRL design to obtain data on a wave rider³ shape in supersonic flow. All configurations were tested to obtain lift and drag data. Additionally, roll moment data were obtained. The test conditions covered a Mach number range of 1.5 through 4.0 at a constant Reynolds number of 15.6×10^6 per metre. Angle of attack variation was from -10° to $+7^\circ$.

A. Equipment

The wind tunnel is a continuous, closed circuit, variable throat tunnel with Mach capability from 1.5 through 5.0 calibrated in 0.25 Mach number increments. The supply pressure can be varied from 250 to 5000 mm Hg. The free stream Reynolds number has a range of 1.6×10^6

1. C. J. Nietubicz, "Some Aerodynamic Characteristics of Supersonic Lifting Bodies," BRL Memorandum Report No. 2458, U.S. Army Ballistic Research Laboratories, Aberdeen Proving Ground, Maryland, March 1975. AD A009704.
2. J. C. McMullen, "Wind Tunnel Testing Facilities at the Ballistic Research Laboratories," BRL Memorandum Report No. 1292, U.S. Army Ballistic Research Laboratories, Aberdeen Proving Ground, Maryland, July 1960. AD 244180.
3. L. F. Crabtree and P. A. Treadgeld, "Experiments on Hypersonic Lifting Bodies," International Council of the Aeronautical Sciences Paper No. 66-24, September 1966.

to 2.8×10^6 per metre for a stagnation temperature of 311° Kelvin. The test section is 0.33 metres wide by 0.38 metres high and the standard angle of attack range is from $+15^\circ$ to -10° . An automatic roll head allows the model to be positioned throughout 270° ($+180^\circ$ to -90°) without interruption of air flow.

A six component strain gage balance was used to measure the aerodynamic forces and moments. The maximum allowable normal and side force acting between the gages are 890 Newtons (N) and 445 N respectively. The associated maximum allowable moments are 34 Newton-meter (Nm) and 14 Nm. The balance capacity in axial force is 334 N and the maximum roll moment is 6.8 Nm.

Due to the unique shape of the configurations tested, the balance was mounted external to the models. A sketch of the model assembly is shown in Figure 1. This arrangement, unfortunately, increases the moment arm causing the maximum allowable loads to be decreased.

The models are shown in Figure 2 and are identified as follows.

<u>Model Description</u>	<u>Configuration No.</u>
E-1 Curved Under Surface	1.00
E-1	2.00
F	3.00
BRL M3 Wave Rider	4.00

B. Test Procedure

All configurations were tested at Mach numbers 1.5, 2.0, 2.5, 3.0, 3.5, and 4.0. The angle of attack variation was from -10° to $+7^\circ$ except where loads began to exceed balance capacities. Base pressures were obtained using 1.6 mm diameter pressure probes located near the model base. Roll moment data were determined at $\phi = 45^\circ$. Spark shadowgraphs and schlieren photographs were obtained throughout the test program.

All data were reduced on the BRL Electronic Scientific Computer (BRLESC) using a standard force reduction program. Strut deflections due to aerodynamic loading were subtracted from the data both in the pitch and yaw planes. Flow corrections were applied to the yaw plane data. Due to the configuration's **asymmetry** with respect to the pitch plane no flow inclination corrections were applied. The coefficients were reduced about a body axis system which was allowed to roll with the model.

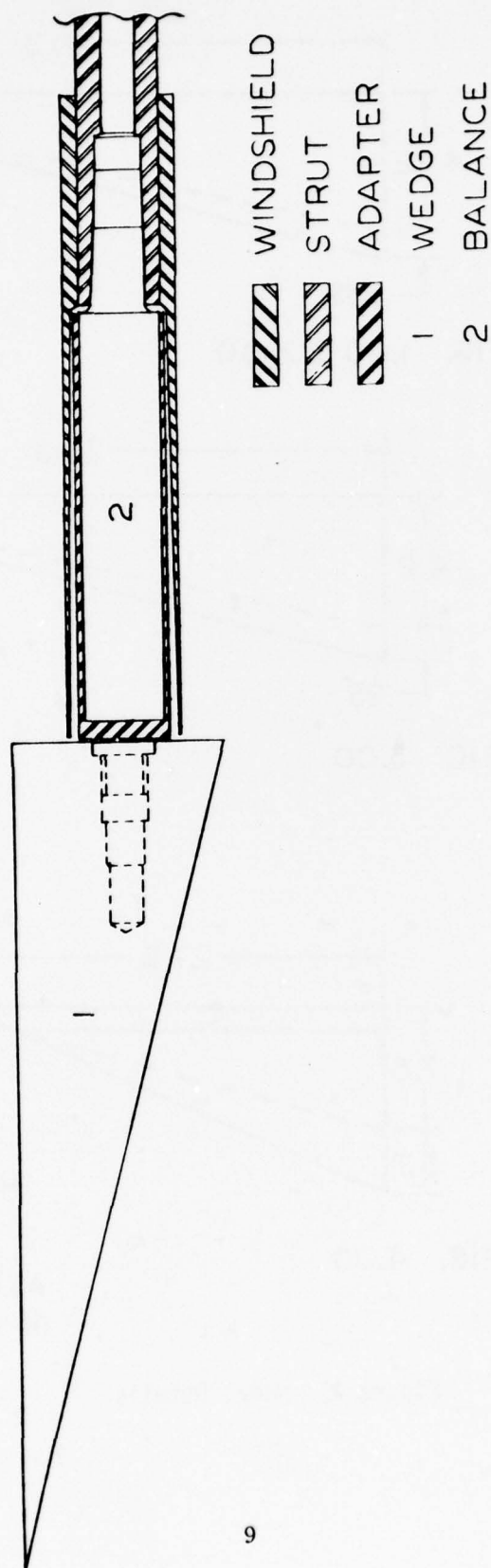
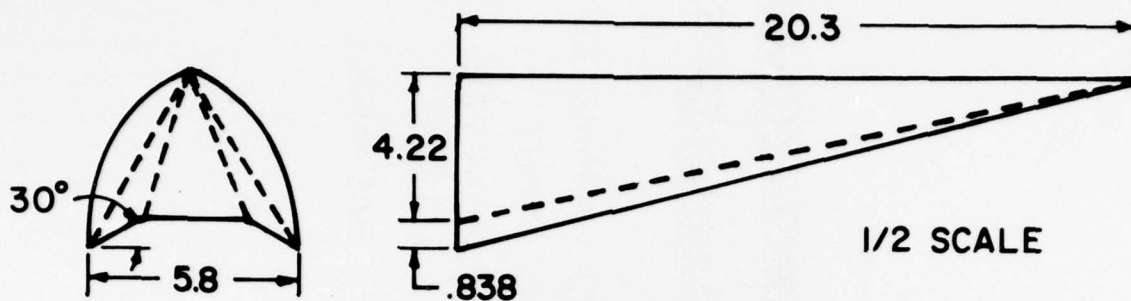
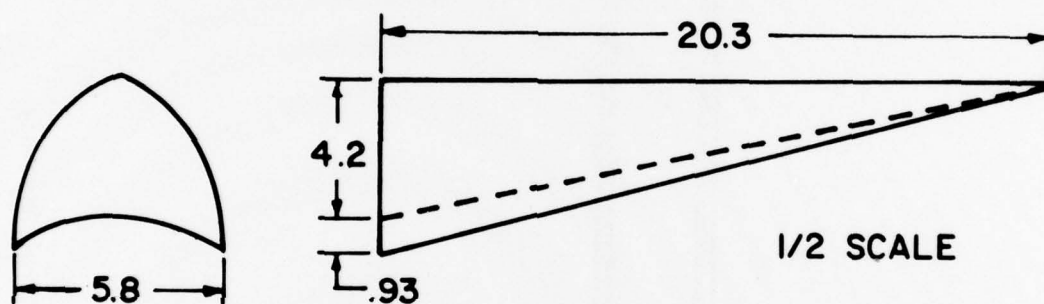


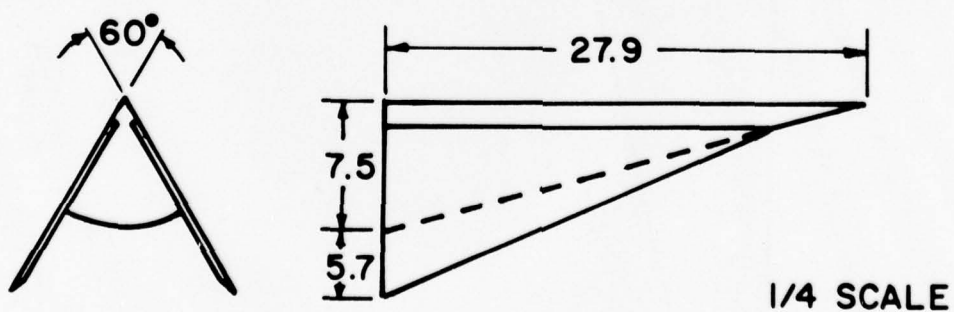
Figure 1. Model 1-Balance-Strut Assembly



CONFIG. 1.00 & 2.00



CONFIG. 3.00



CONFIG. 4.00

ALL DIMENSIONS
IN CENTIMETERS

Figure 2. Model Details

C. Presentation of Data

The reduced data in coefficient form are presented in Appendix A. The normal force (C_N), pitching moment (C_M), axial force (C_A), and normal force center of pressure (X_{CP}) are plotted as a function of angle of attack in Figure A1. Figure A2 shows the same coefficients cross plotted with respect to configuration. The side force (C_Y), yawing moment (C_{YM}), and side force center of pressure (Y_{CP}) are plotted in Figure A3. Configurational variations of the same coefficients are presented in Figure A4. Roll moment data at $\phi = 45^\circ$ are shown in Figure A5 for each configuration. The lift (C_L), drag (C_D), and lift/drag ratio (C_L/C_D) are plotted in Figures A6 and A7.

The normal force and pitching moment slopes were calculated about the point where C_N becomes zero and are tabulated in Table I for each configuration.

III. DISCUSSION

The data for configurations 1.00, 2.00, and 3.00 show characteristically similar patterns to that reported previously¹. The normal force data are nonlinear above $\alpha = 0^\circ$ and are effectively independent of Mach number variation. Configuration 4.00 (Figure A1d), however, shows a strong Mach number dependence above $\alpha = -5^\circ$. Common to all configurations was the expected increase in axial force with decreasing Mach number and the invariance of normal force center of pressure with respect to Mach number and angle of attack. The normal force center of pressure is calculated using the normal force coefficient; therefore, the apparent discontinuity in X_{CP} is due to the normal force going to zero at that point. Figure A2 shows the effect of configuration at each test Mach number. For all Mach numbers, the results for configuration 4.00 show a higher normal force coefficient and lower axial force coefficient in comparison with the other configurations. The difference in normal force and axial force data becomes smaller as the Mach number increases. This can be seen in Figures A2a through A2f. The axial force data at Mach 1.5 was invalid for configuration 4.00 due to unsteady flow conditions caused by the relatively large model size.

The side force data presented in Figures A3 and A4 are symmetrical with respect to $\alpha = 0^\circ$. The side force center of pressure is again invariant with respect to Mach number and angle of attack. The side force data for configuration 4.00 (Figure A3d) shows a slight variation with Mach number. The data scatter of Y_{CP} for configuration 3.00 at Mach number 4.0 is peculiar to that one run and is most probably caused by erroneous raw data.

Roll moment data were obtained for negative angle of attack only, since the important regime for this test series was centered around the trim angle of approximately -7° . A negative roll moment coefficient (counter clockwise direction) is considered as the restoring moment throughout this discussion. The roll moment data for configurations 1.00, 2.00, and 3.00 as seen in Figures A5a through A5c are small and can be considered negligible in terms of a restoring moment. However, it is interesting to note that the roll moment data for all configurations is a restoring type moment whereas the previously reported data showed non-restoring roll moments for $\alpha < 0^\circ$. Since the shapes are not appreciably different, the change in sign for roll moment data is not completely understood. The roll moment data of configuration 4.00, seen in Figure A5d, shows a significant increase in magnitude for roll moment over all previously tested configurations. Although only a few wave rider type shapes have been tested at supersonic speeds, the increased restoring roll moment may be a characteristic.

The data were also reduced to obtain lift and drag coefficients. A comparison of lift/drag for configurations 1.00, 2.00, and 3.00 are shown in Figures A6a through A6c to be dependent on Mach number. A maximum value of approximately 2.5 was attained near $\alpha = 6^\circ$. Conversely, there was no Mach number dependence for configuration 4.00 as can be seen in Figure A6d. The maximum value of lift/drag for this configuration was 3.0 at $\alpha = 1^\circ$. Configuration 4.00 was designed to be consistent with the wave rider theory; however, concessions made during model fabrication introduced the edge discontinuity. It was felt that this change would not significantly alter the planar shock pattern. However, as can be seen in the spark shadowgraph (Figure 3) the shock is slightly below the model.

A comparison of previous configurations with those reported here is presented in Figure 4 in the form of lift/drag data. Configurations 972.00 and 4.00 which are nearest to a wave rider design have the largest magnitudes of lift/drag for all angles and a more negative trim angle. The area of concern is most likely not with large values of lift/drag but most probably with the configuration which produces the largest lift slope (C_{L_α}) near trim since the thought is to fly

these shapes near the trim conditions. Table I is a tabulation of summary data which includes $C_{L_\alpha(\text{trim})}$. Configuration 4.00 exhibits

the highest slope for all Mach numbers with the exception of Mach 4.0.

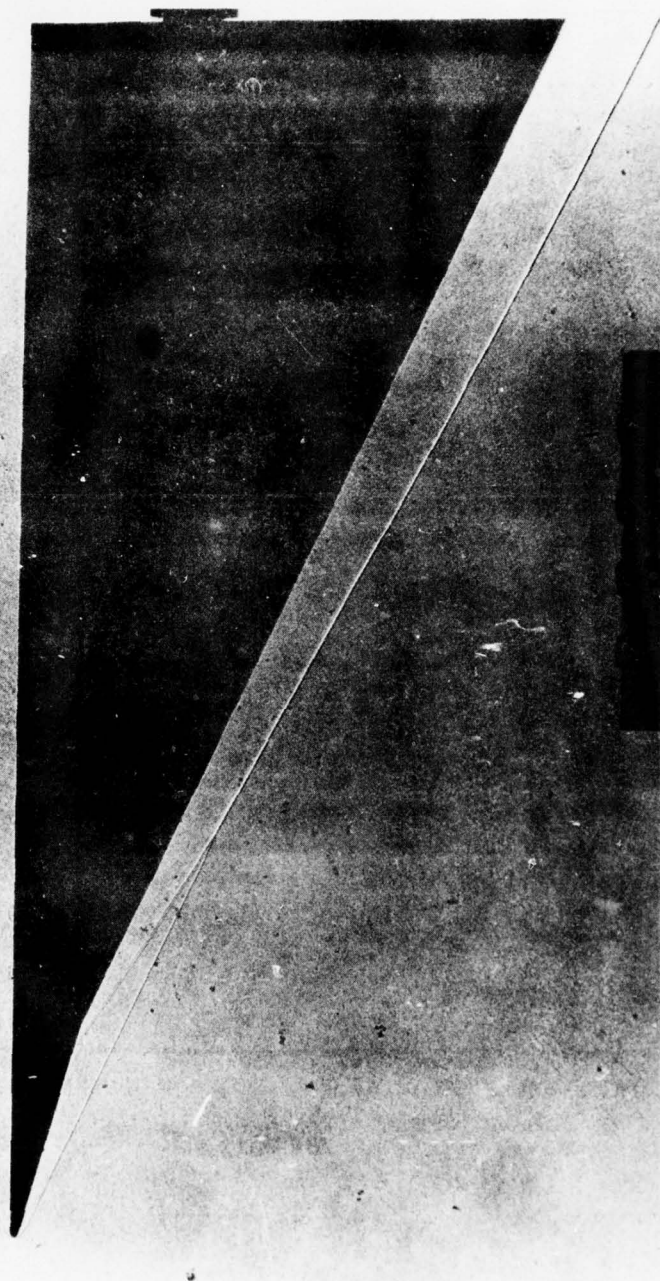


Figure 3. Spark Shadowgraph, $M = 3.0$, $\alpha = 0^\circ$, $CONFIG = 4.00$

The figure is a scatter plot with 'LIFT/DRAG' on the vertical axis and 'ALPHA' on the horizontal axis. The vertical axis has major tick marks at -1.0, -0.5, 0, 0.5, 1.0, 1.5, 2.0, 2.5, 3.0, 3.5, and 4.0. The horizontal axis has major tick marks at -10.0, -8.0, -6.0, -4.0, -2.0, 0, 2.0, 4.0, 6.0, 8.0, 10.0, and 12.0. The data points are labeled with letters (X, O, B, V, W, Y, Z) and numbers (1.00, 2.00, 3.00, 4.00, 972.80, 972.60, 972.00). The points are distributed across the plot, showing a general trend of decreasing Lift/Drag as Alpha increases. There are also points at negative Alpha values, showing a peak in Lift/Drag around Alpha = -4.0.

14

Table I. Summary Data

<u>CONFIG</u>	<u>M</u>	<u>C_{N_α}</u>	<u>C_{M_α}</u>	<u>C_{L_α}(trim)</u>
1.00	1.5	.0187	.0061	.0167
	2.0	.0180	.0059	.0165
	2.5	.0176	.0057	.0164
	3.0	.0169	.0055	.0159
	3.5	.0161	.0053	.0156
	4.0	.0158	.0051	.0155
2.00	1.5	.0180	.0060	.0157
	2.0	.0183	.0060	.0167
	2.5	.0177	.0058	.0165
	3.0	.0170	.0056	.0161
	3.5	.0165	.0054	.0159
	4.0	.0161	.0052	.0157
3.00	1.5	.0182	.0060	.0164
	2.0	.0180	.0059	.0167
	2.5	.0176	.0057	.0164
	3.0	.0168	.0054	.0159
	3.5	.0165	.0052	.0158
	4.0	.0158	.0051	.0152
4.00	1.5	.0269	.0079	.0268
	2.0	.0243	.0072	.0237
	2.5	.0217	.0065	.0207
	3.0	.0194	.0059	.0192
	3.5	.0175	.0054	.0168
	4.0	.0160	.0054	.0154

IV. CONCLUSIONS

Four additional lifting body configurations have been tested at supersonic speeds. The lift/drag data for three configurations were found to be dependent on Mach number while the wave rider like shape showed no Mach number dependence. For all configurations, the position of the normal force center of pressure was found to be invariant with respect to Mach number and angle of attack. The maximum value of lift/drag was found to be 3.0 for the pseudo wave rider configuration, which also exhibited the largest lift slope near trim.

The roll moment data continues to reveal the problem of an almost non-existent restoring moment for these configurations. The wave rider like shape, however, does show a measurable restoring moment.

APPENDIX A
Aerodynamic Coefficients

COPY AVAILABLE TO DCS DOES NOT
PERMIT FULLY LEGIBLE REPRODUCTION

BEST AVAILABLE COPY

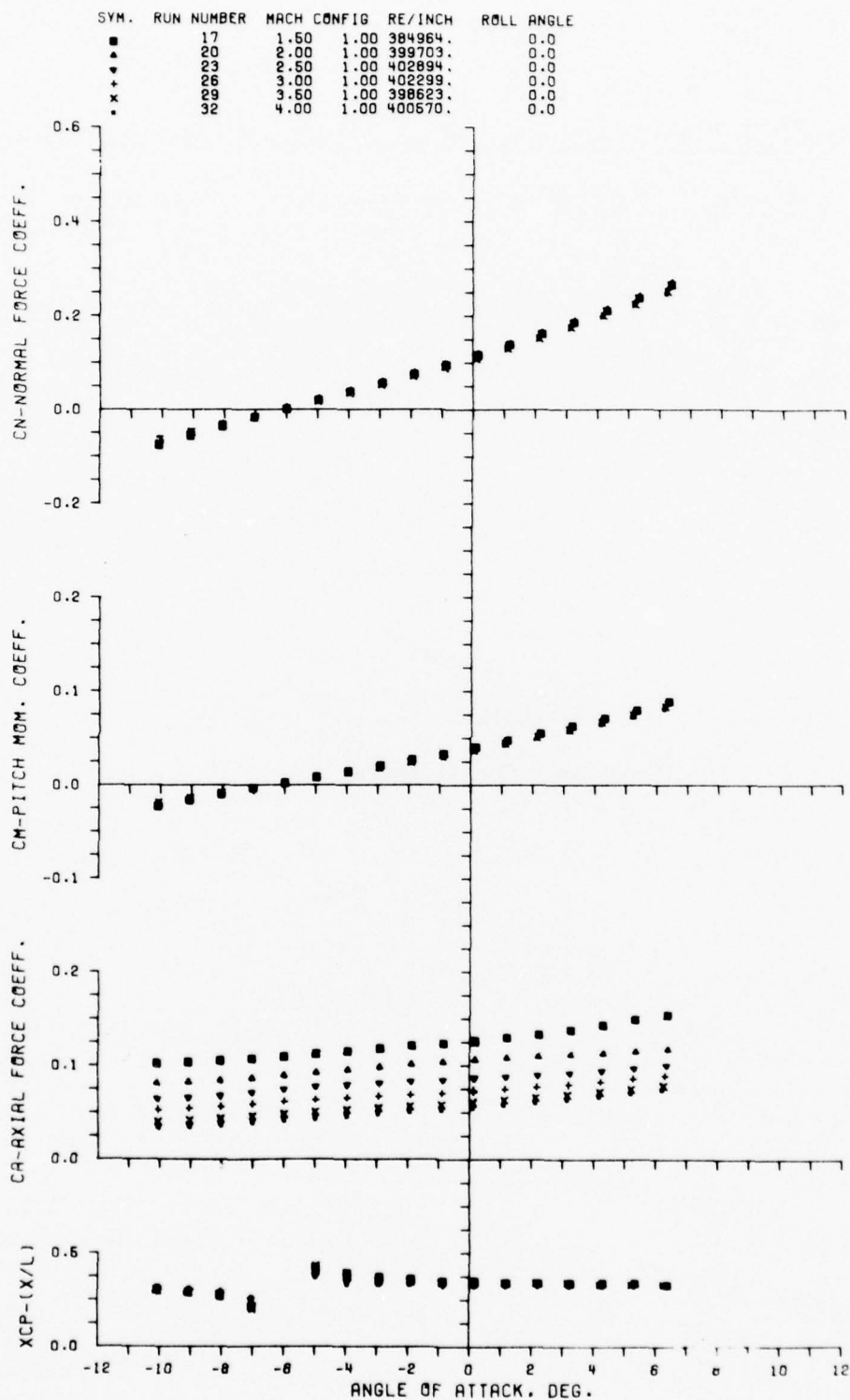
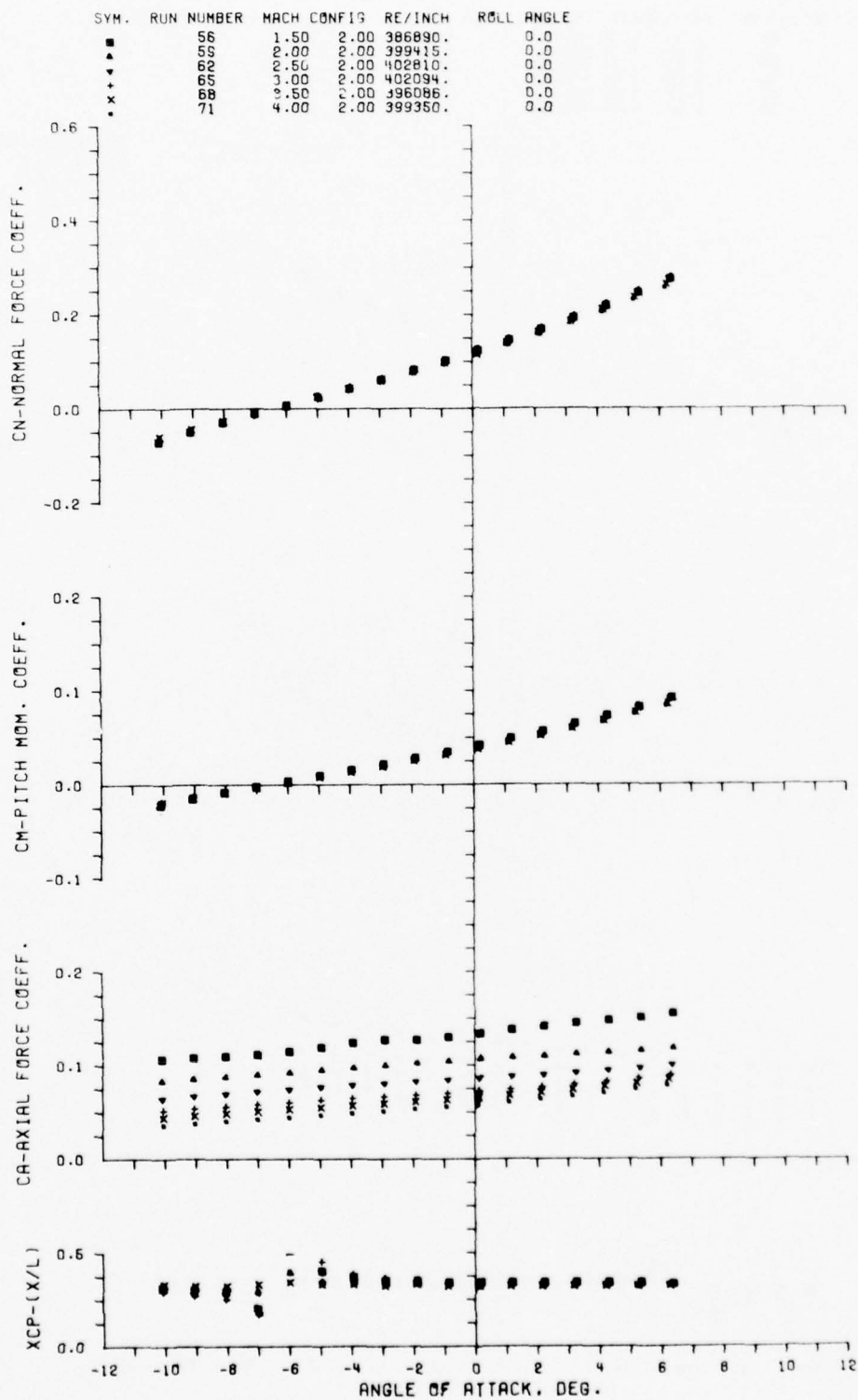
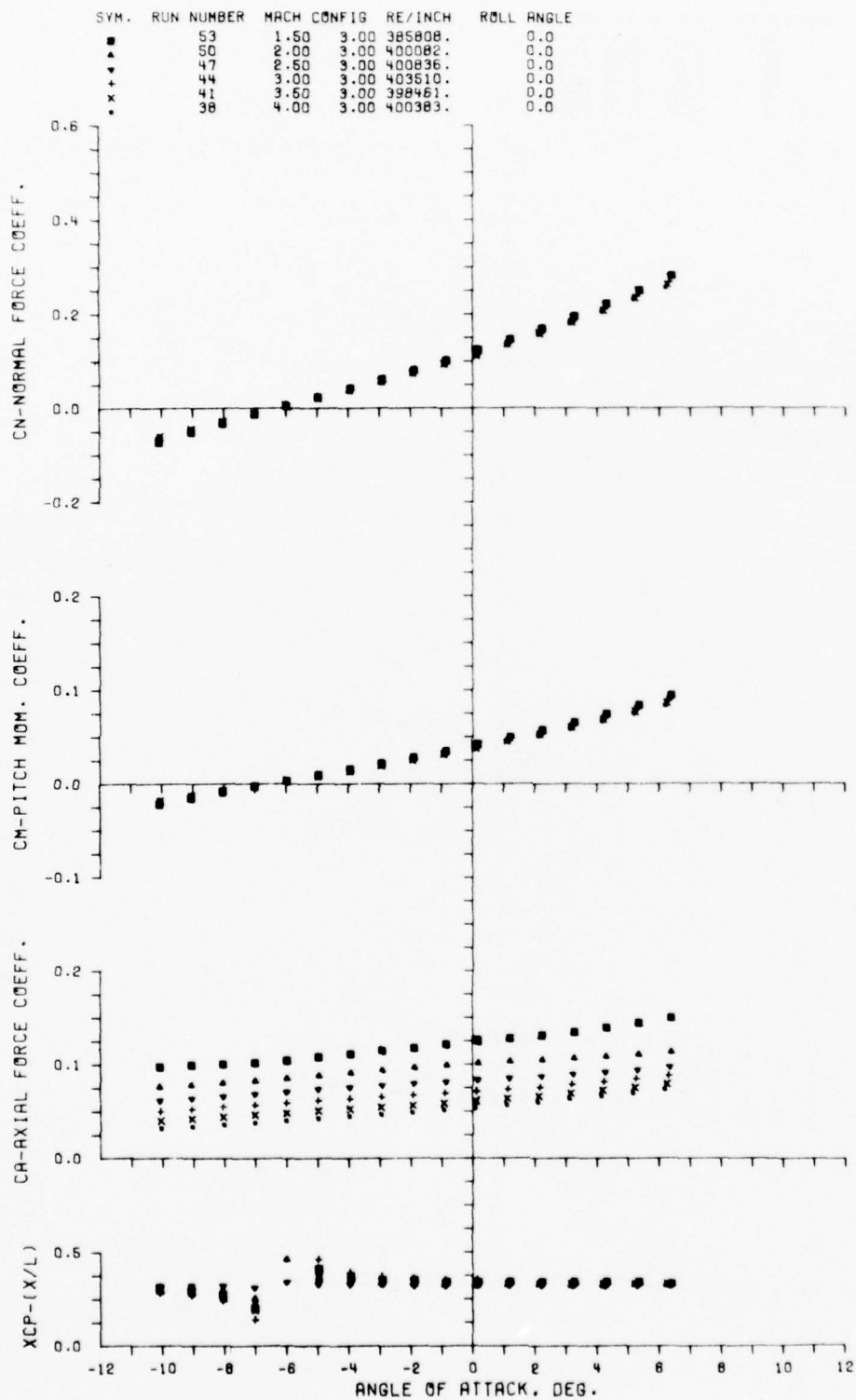


Figure A1. Aerodynamic Coefficients C_N , C_M , C_A , X_{CP} --
Mach Number Variation
a. CONFIG 1.00

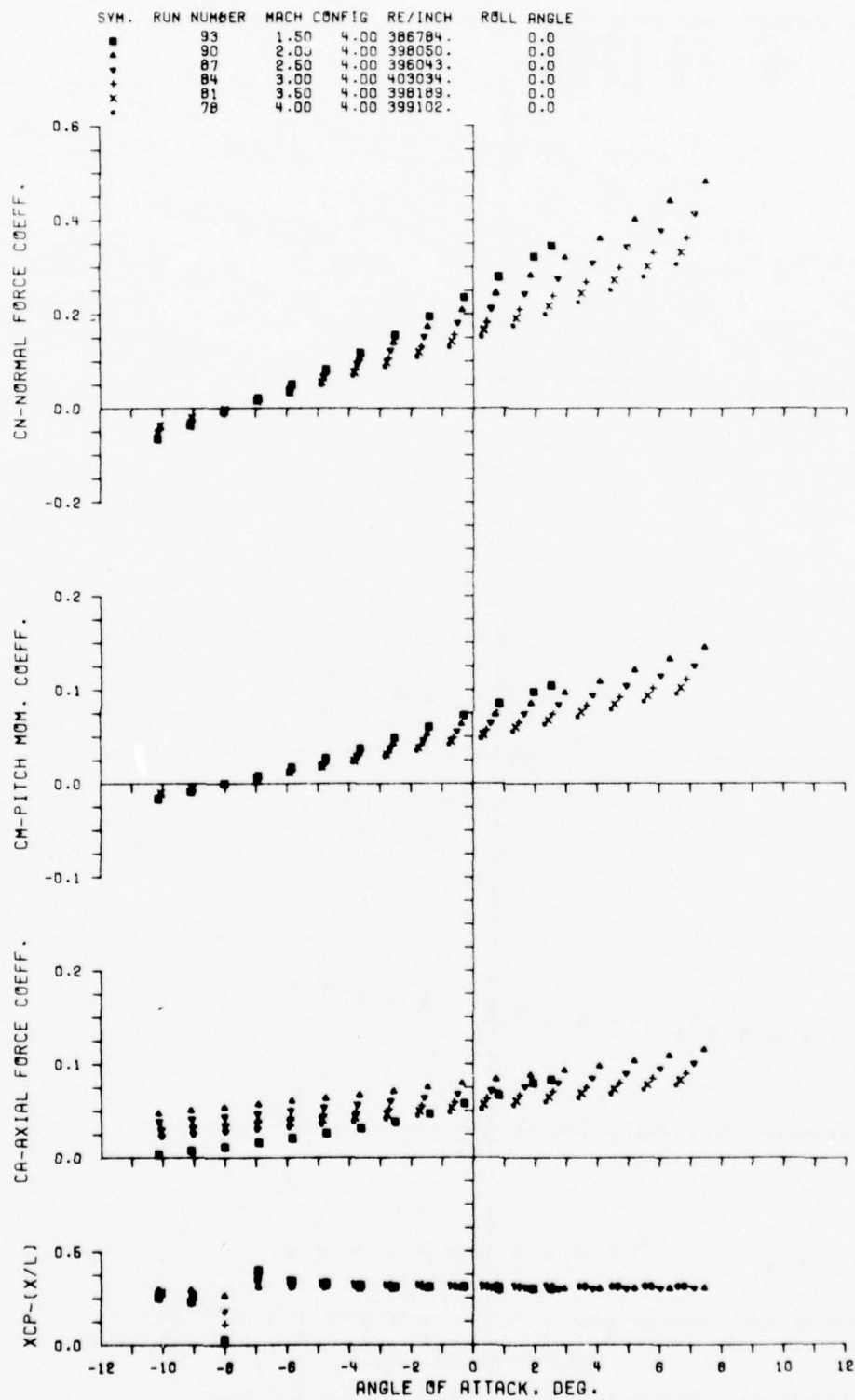


BEST AVAILABLE COPY

BEST AVAILABLE COPY



BEST AVAILABLE COPY



BEST AVAILABLE COPY

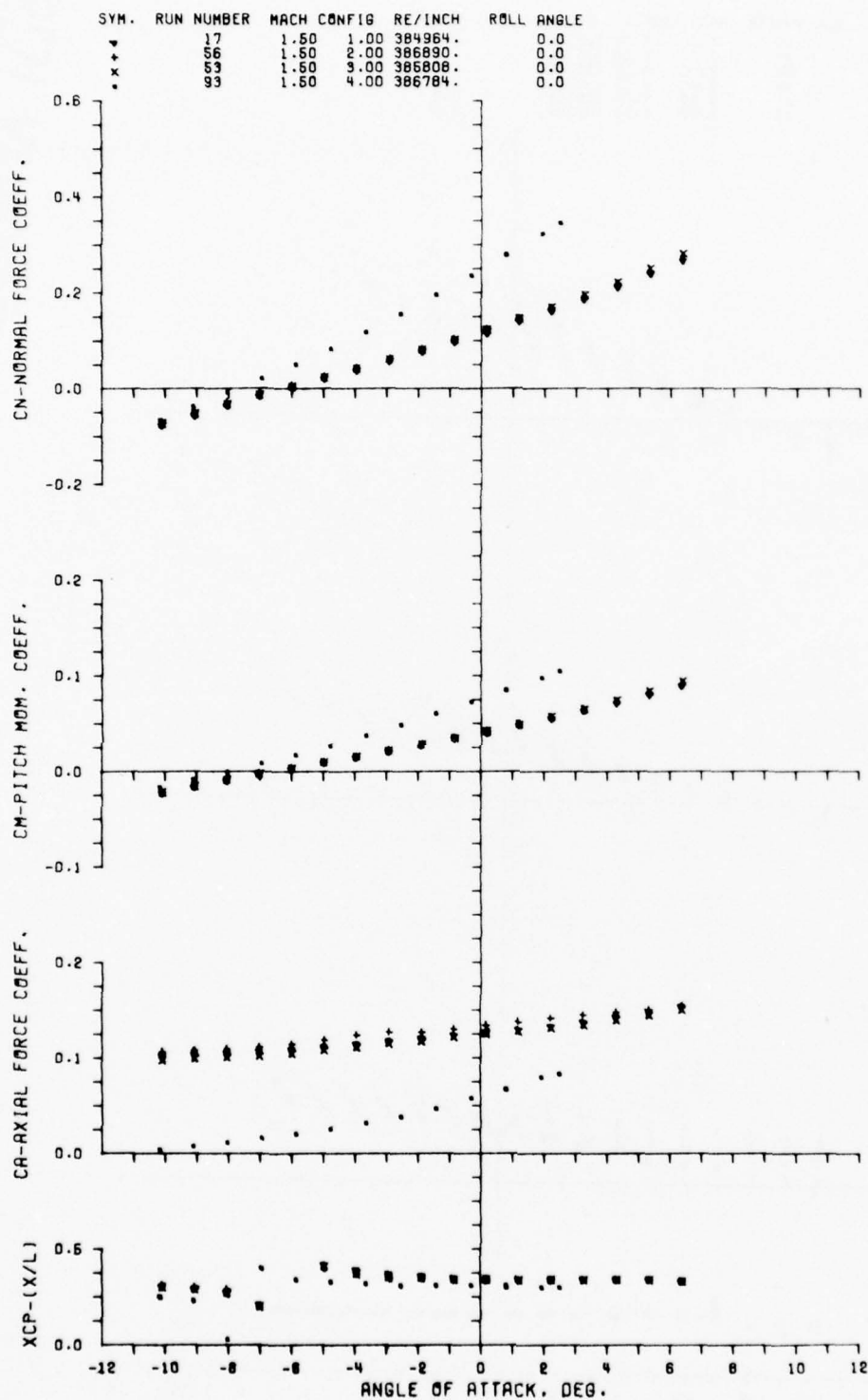
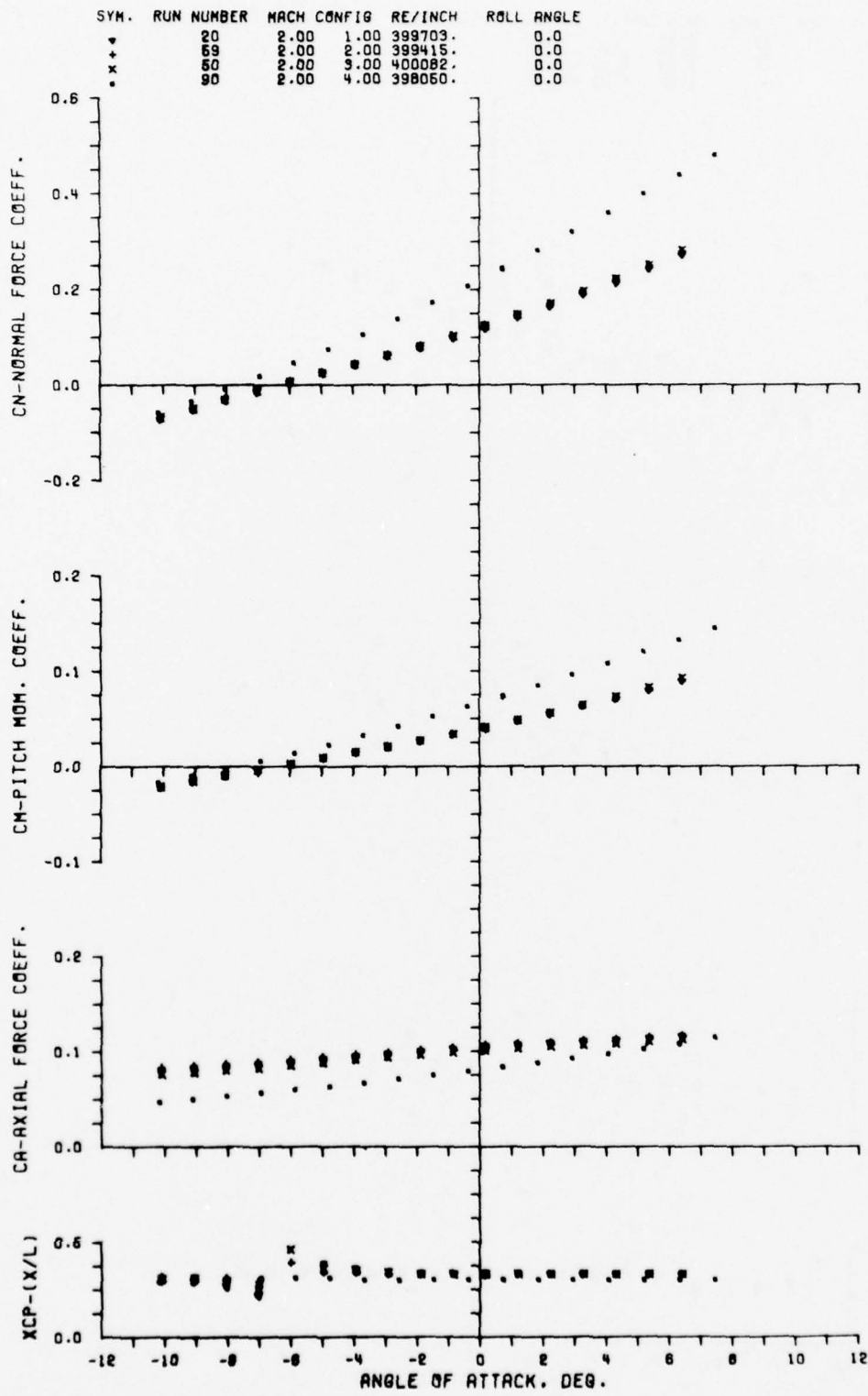


Figure A2. Aerodynamic Coefficients C_N , C_M , C_A , X_{CP} --
Configuration Variation

a. MACH 1.5



BEST AVAILABLE COPY

Figure A2. Continued

b. MACH 2.0

SYM. RUN NUMBER MACH CONFIG RE/INCH ROLL ANGLE
 23 2.50 1.00 402894. 0.0
 52 2.50 2.00 402810. 0.0
 47 2.50 3.00 400836. 0.0
 87 2.50 4.00 396043. 0.0

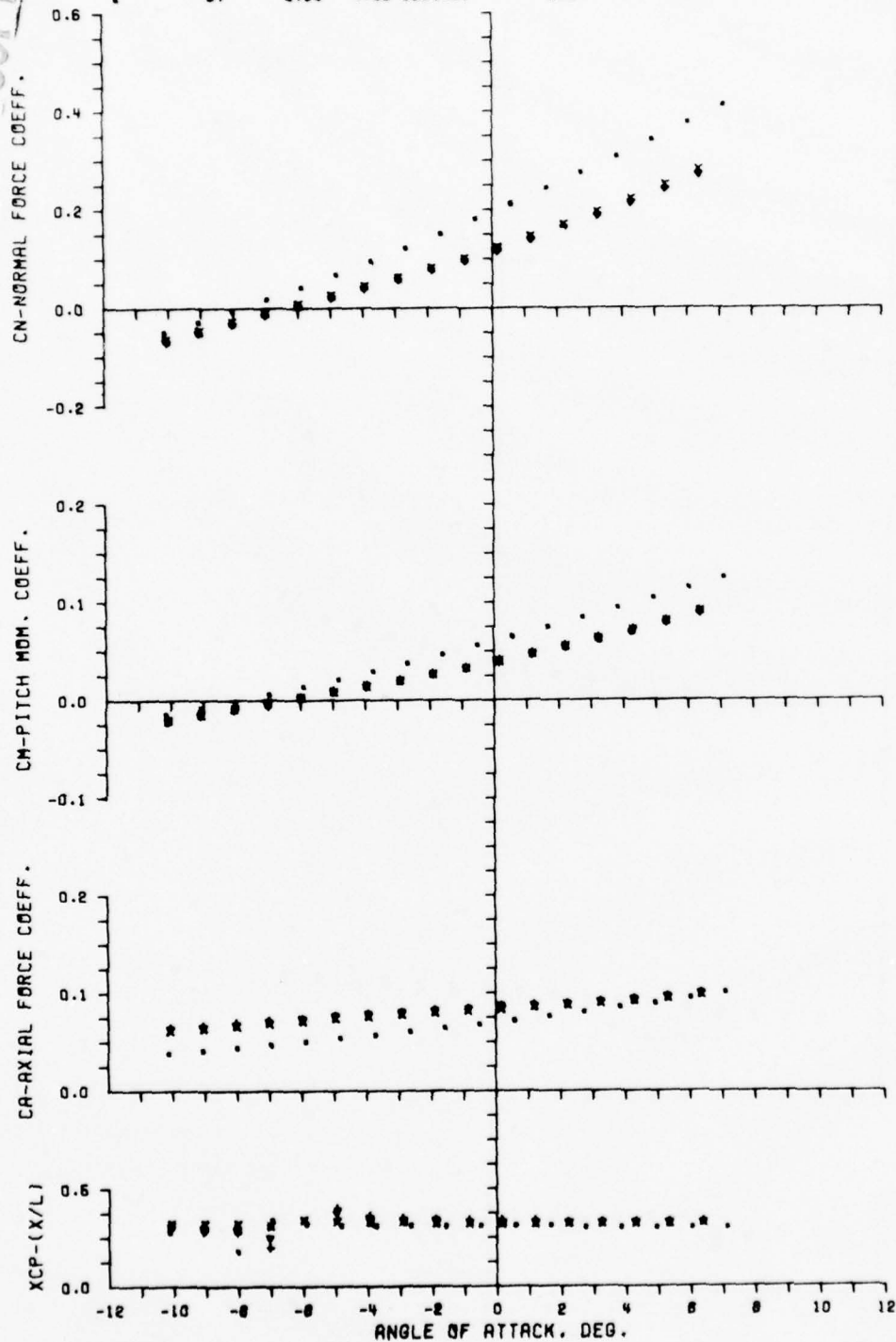
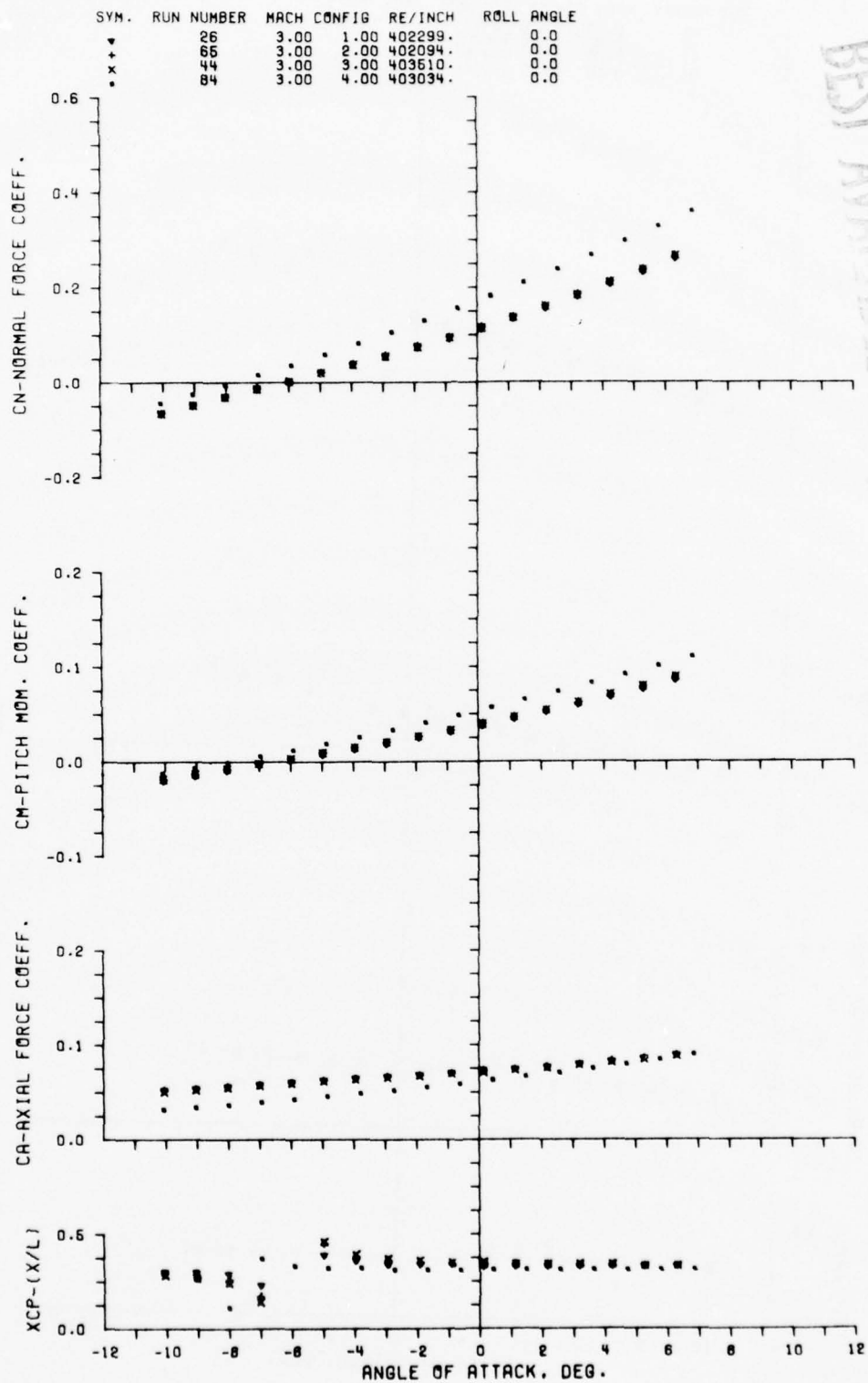


Figure A2. Continued

c. MACH 2.5



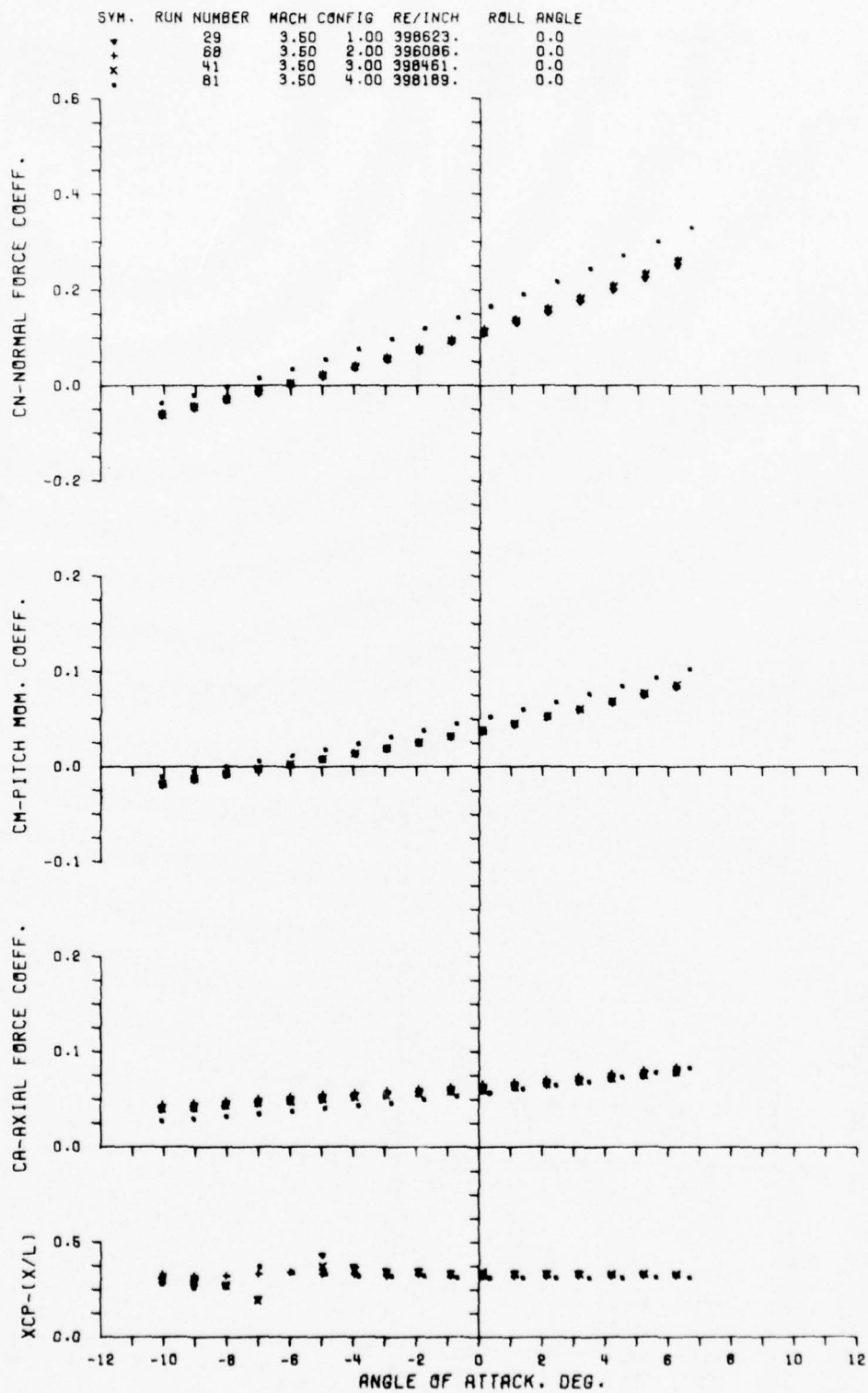


Figure A2. Continued

e. MACH 3.5

SYM.	RUN NUMBER	MACH	CONFIG	RE/INCH	ROLL ANGLE
▼	32	4.00	1.00	400570.	0.0
+	71	4.00	2.00	399350.	0.0
x	38	4.00	3.00	400383.	0.0
.	78	4.00	4.00	399102.	0.0

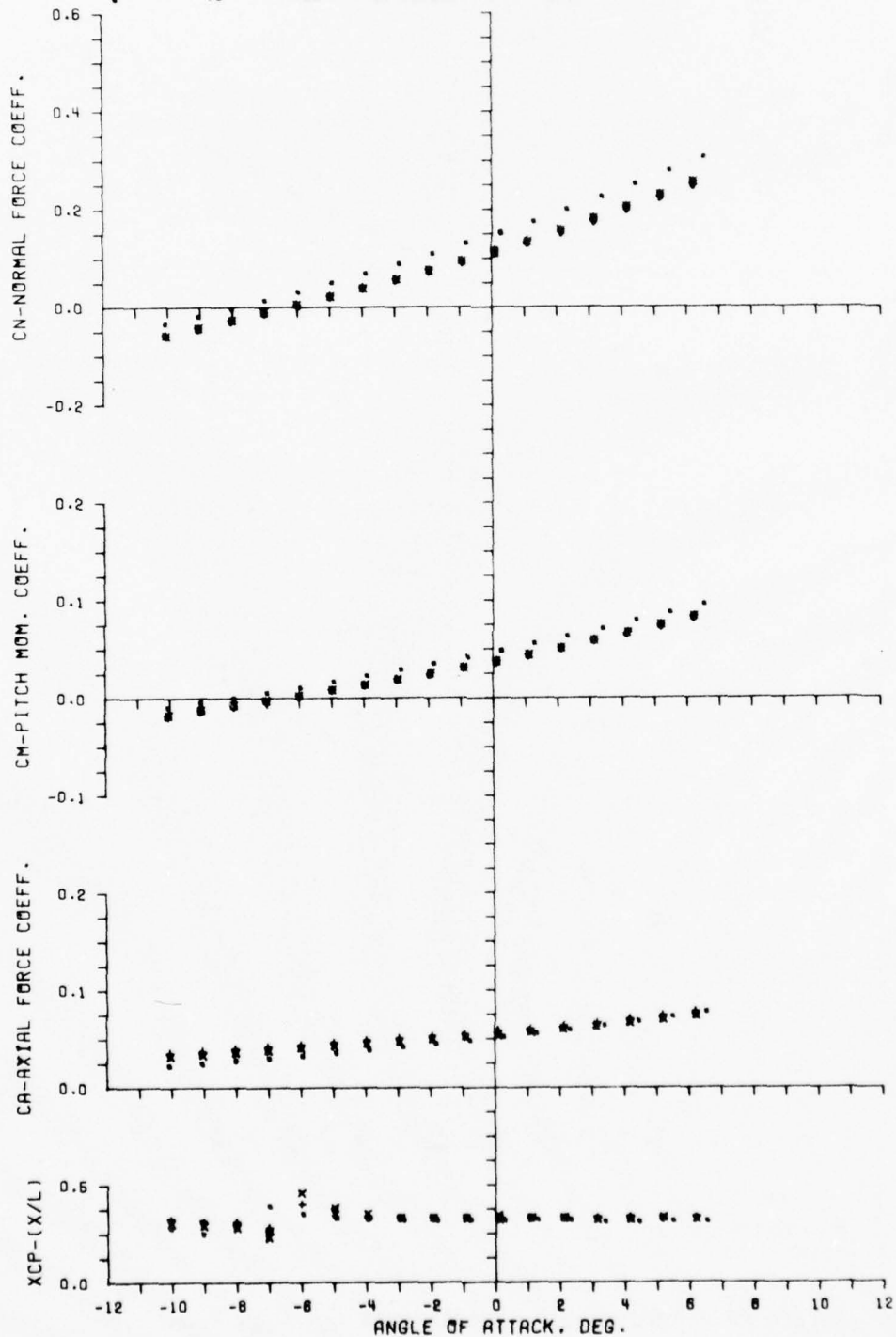


Figure A2. Concluded

f. MACH 4.0

BEST AVAILABLE COPY

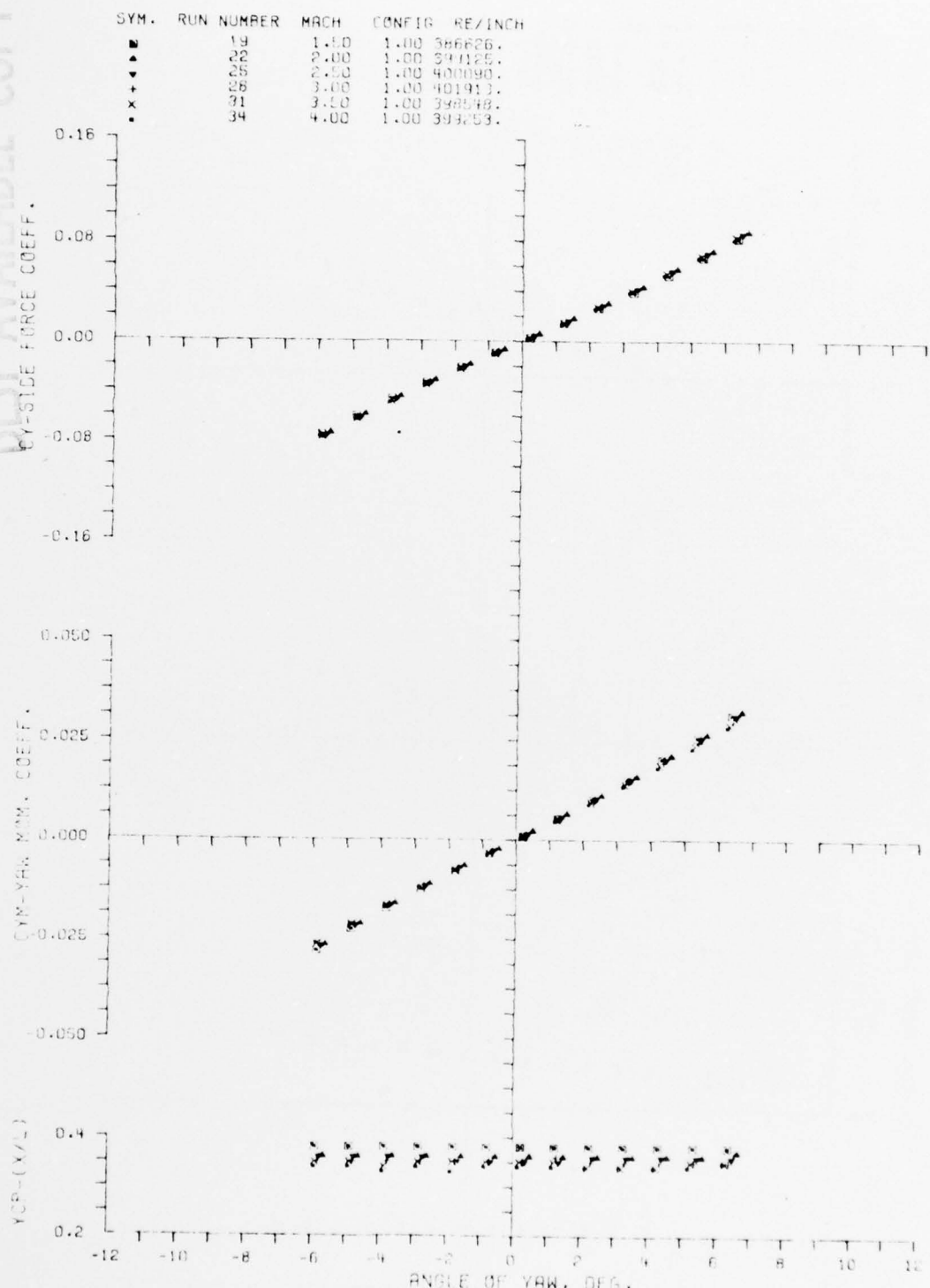


Figure A3. Aerodynamic Coefficients C_Y , C_{YM} , Y_{CP} --
Mach Number Variation

a. CONFIG 1.00

BEST AVAILABLE COPY

SYM.	RUN NUMBER	MACH	CONFIG	REF INCH
■	58	1.50	2.00	367496.
▲	61	2.00	2.00	399316.
▼	64	2.50	2.00	403109.
+	67	3.00	2.00	402102.
x	70	3.50	2.00	398616.
.	73	4.00	2.00	399118.

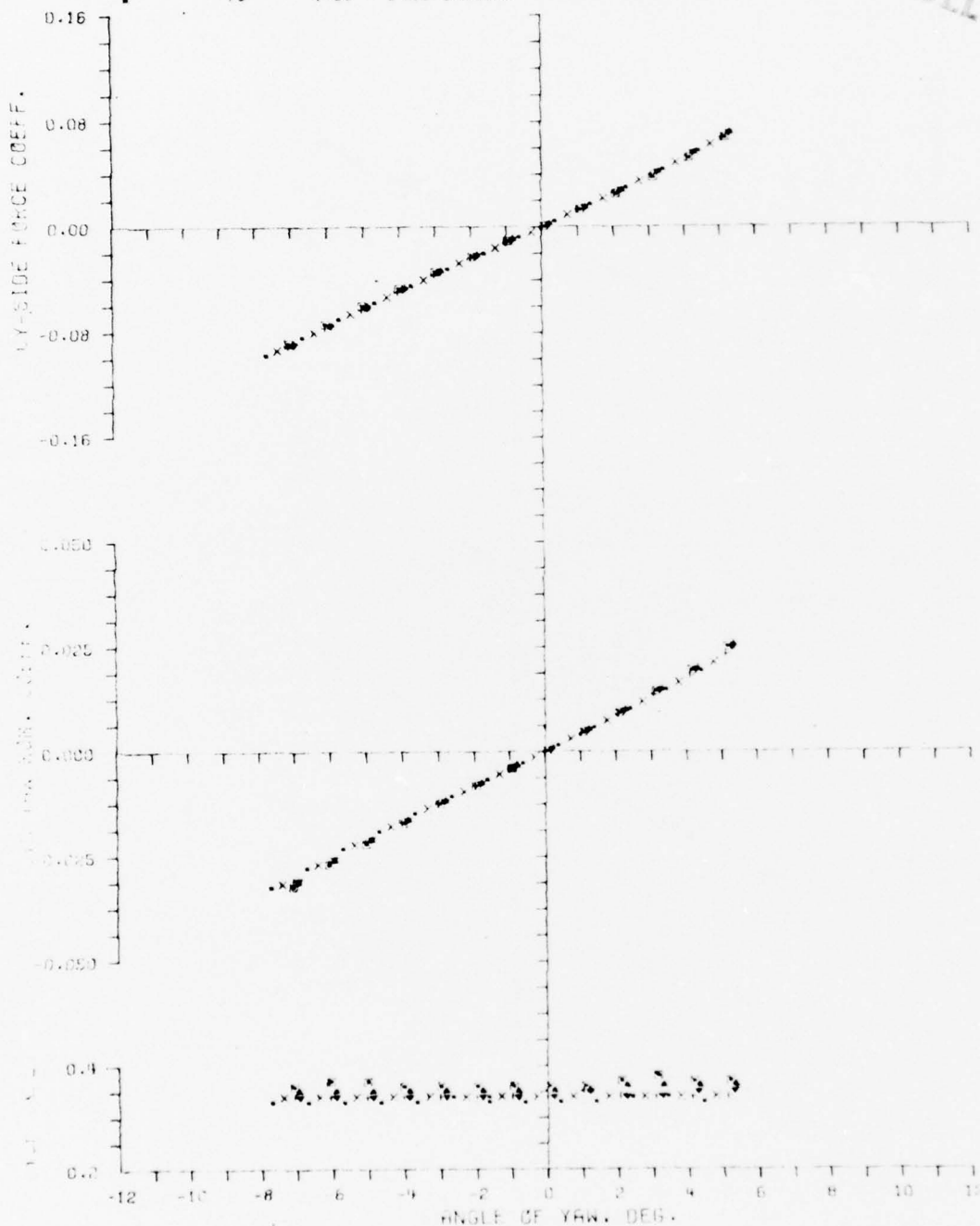
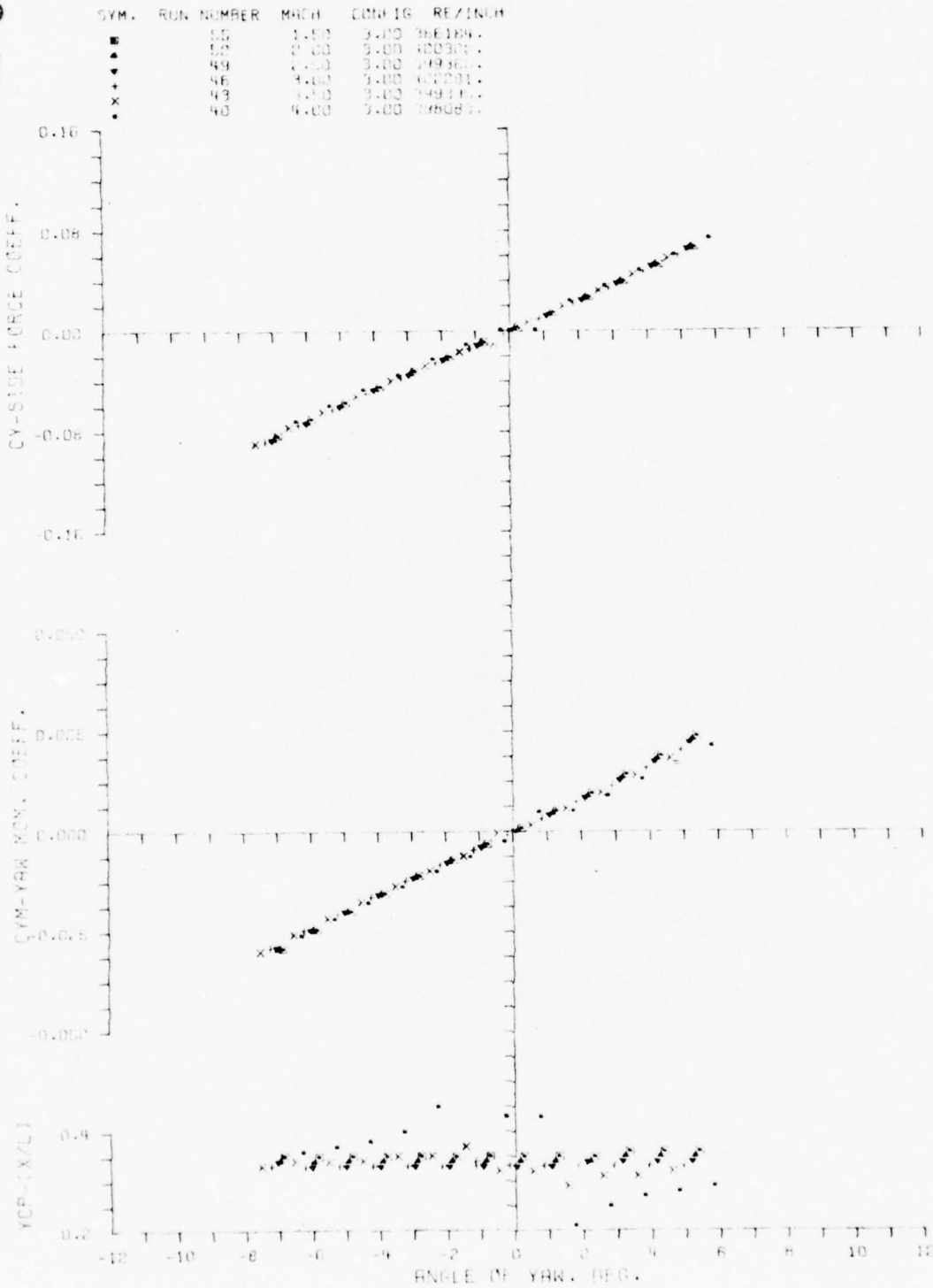


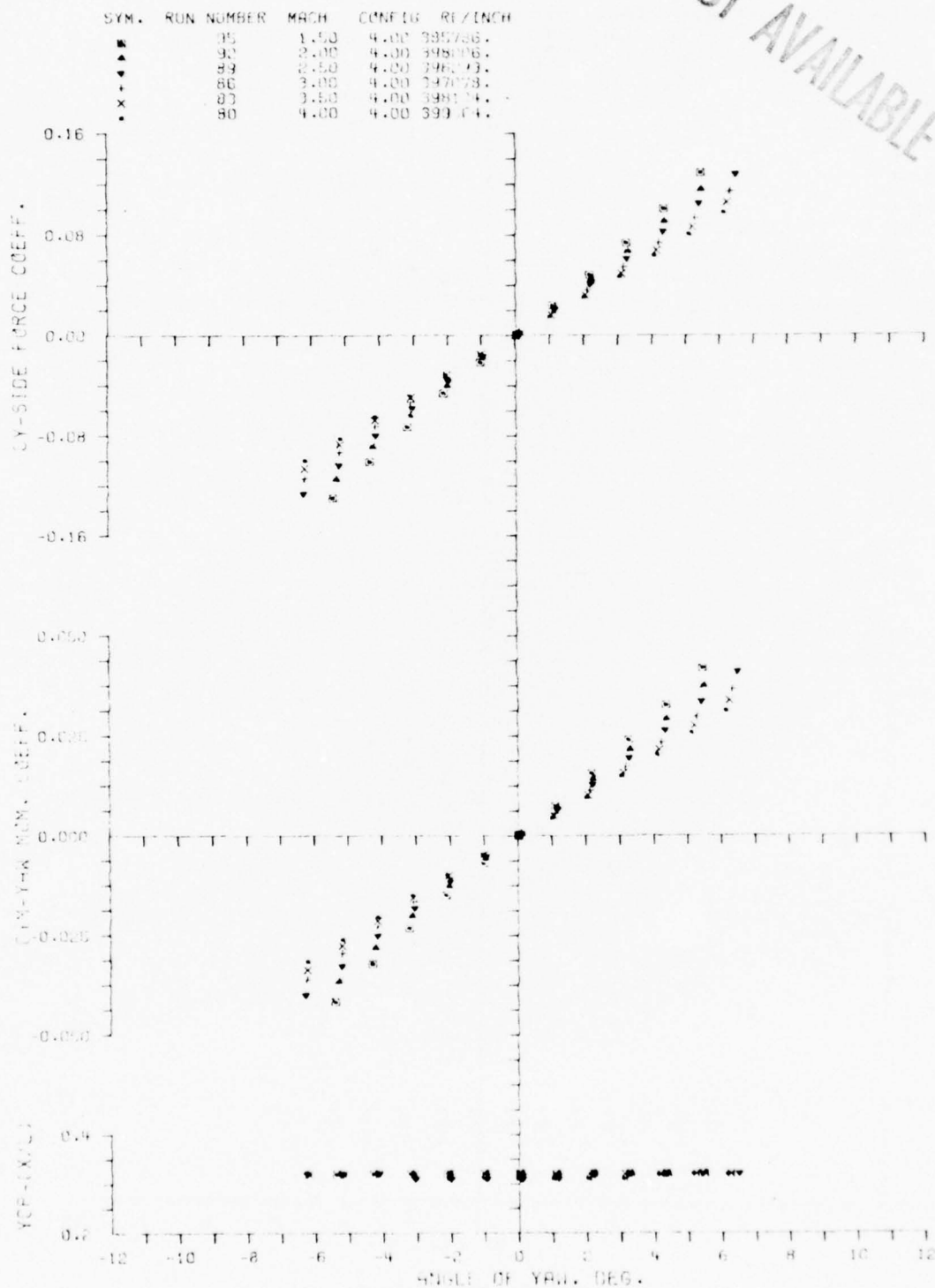
Figure A3. Continued

b. CONFIG 2.00

BEST AVAILABLE COPY



BEST AVAILABLE COPY



BEST AVAILABLE COPY

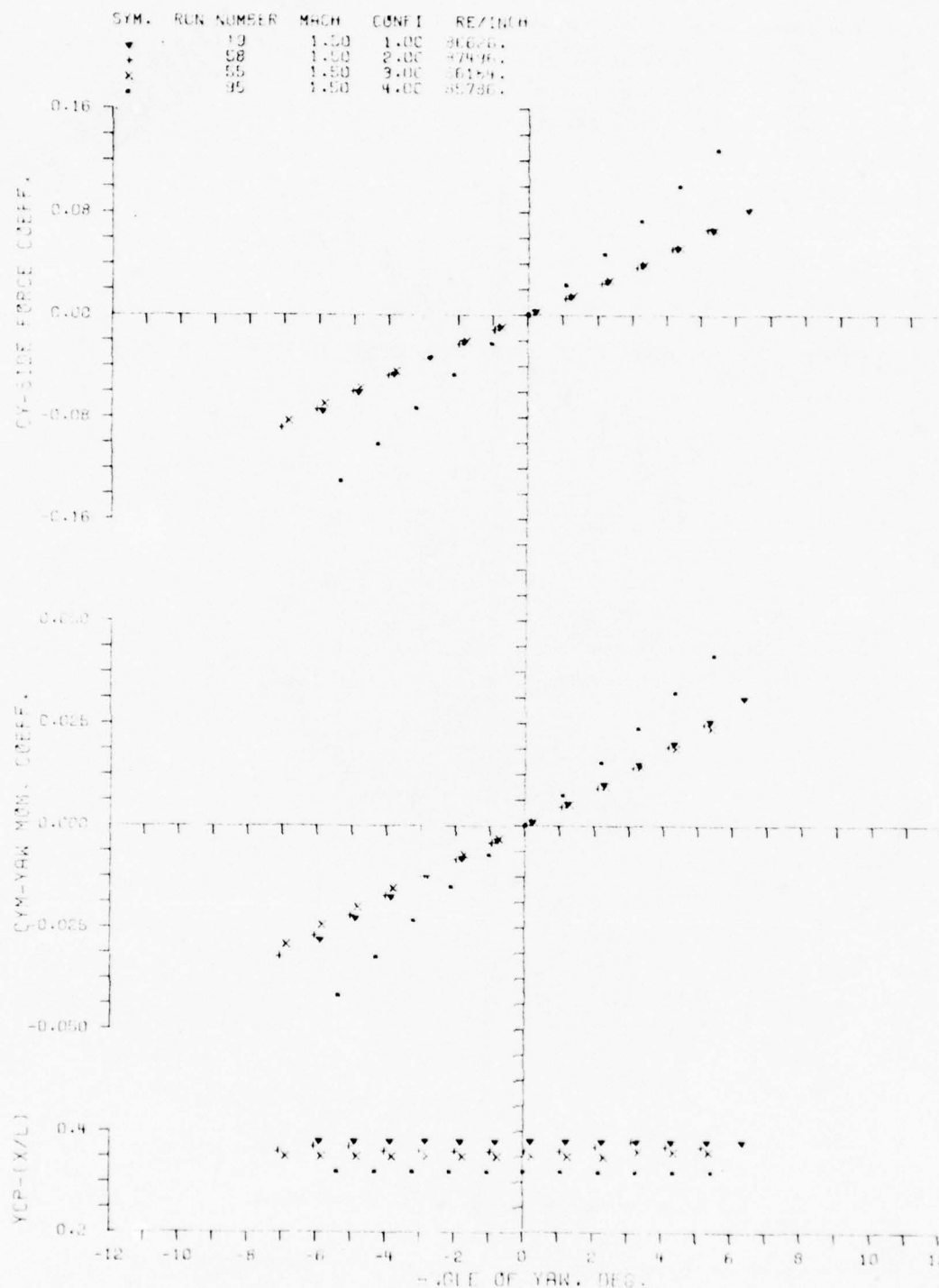


Figure A4. Aerodynamic Coefficients C_Y , C_{YM} , Y_{CP} --
Configuration Variation

a. MACH 1.5

BEST AVAILABLE COPY

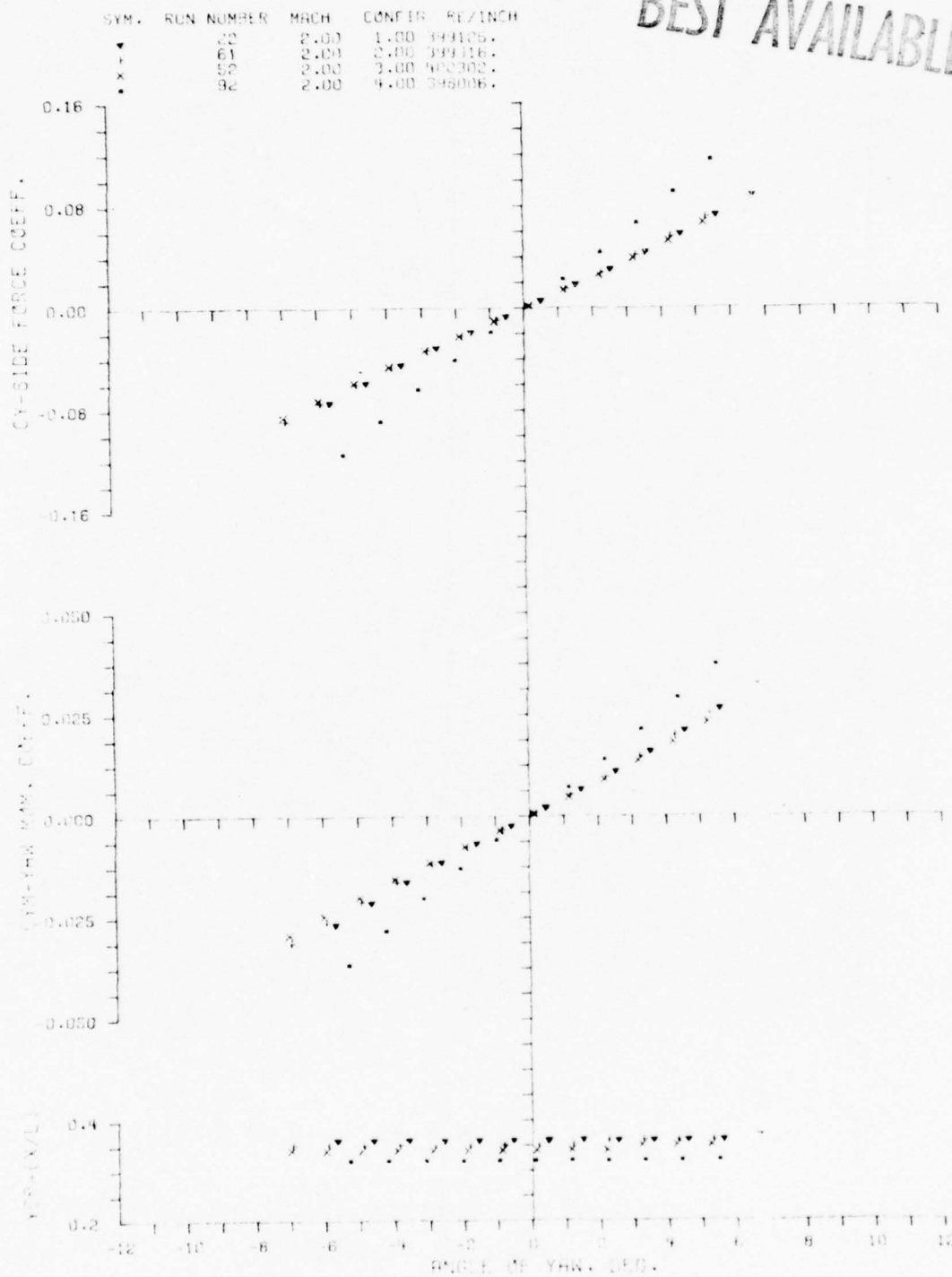
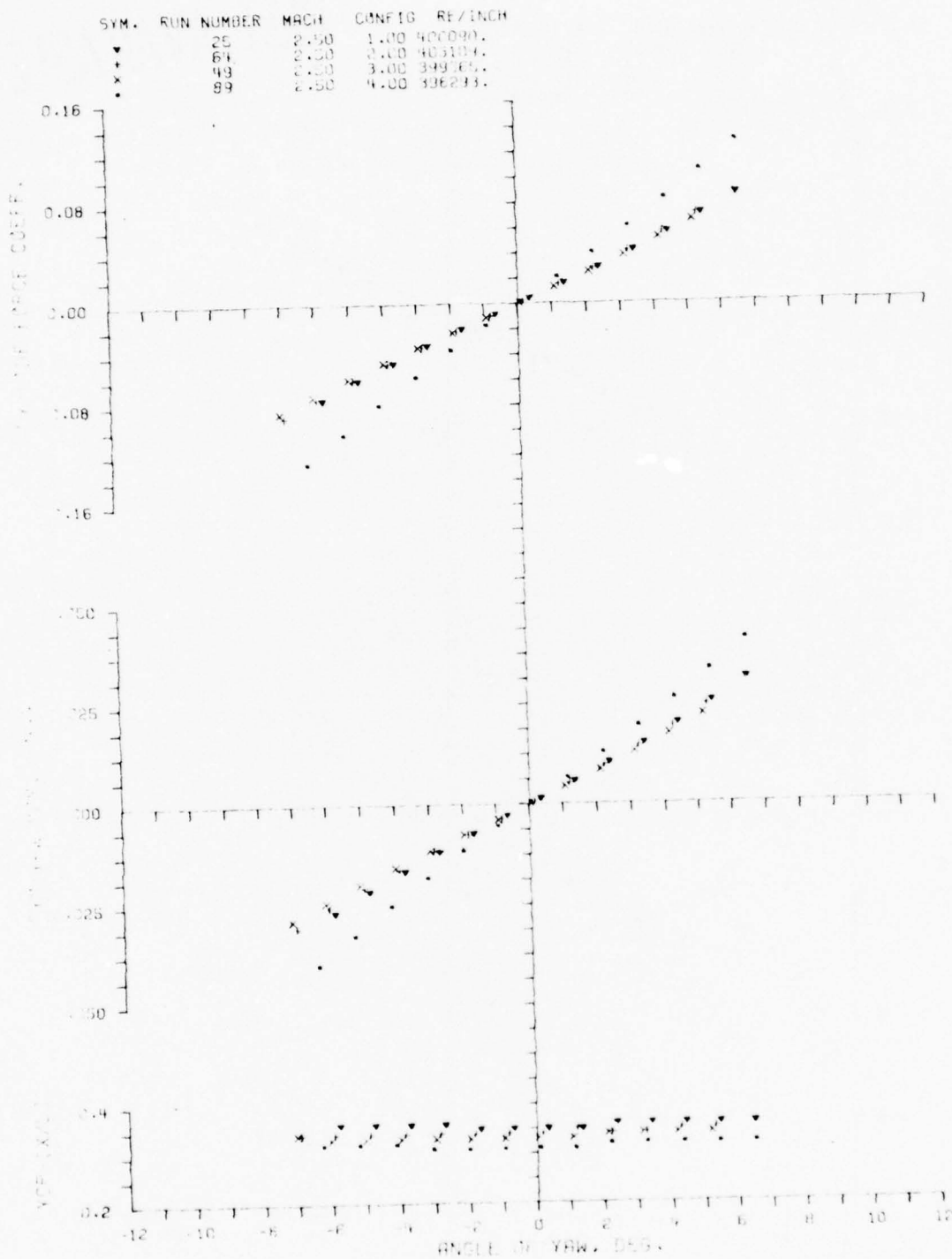


Figure A4. Continued

b. MACH 2.0



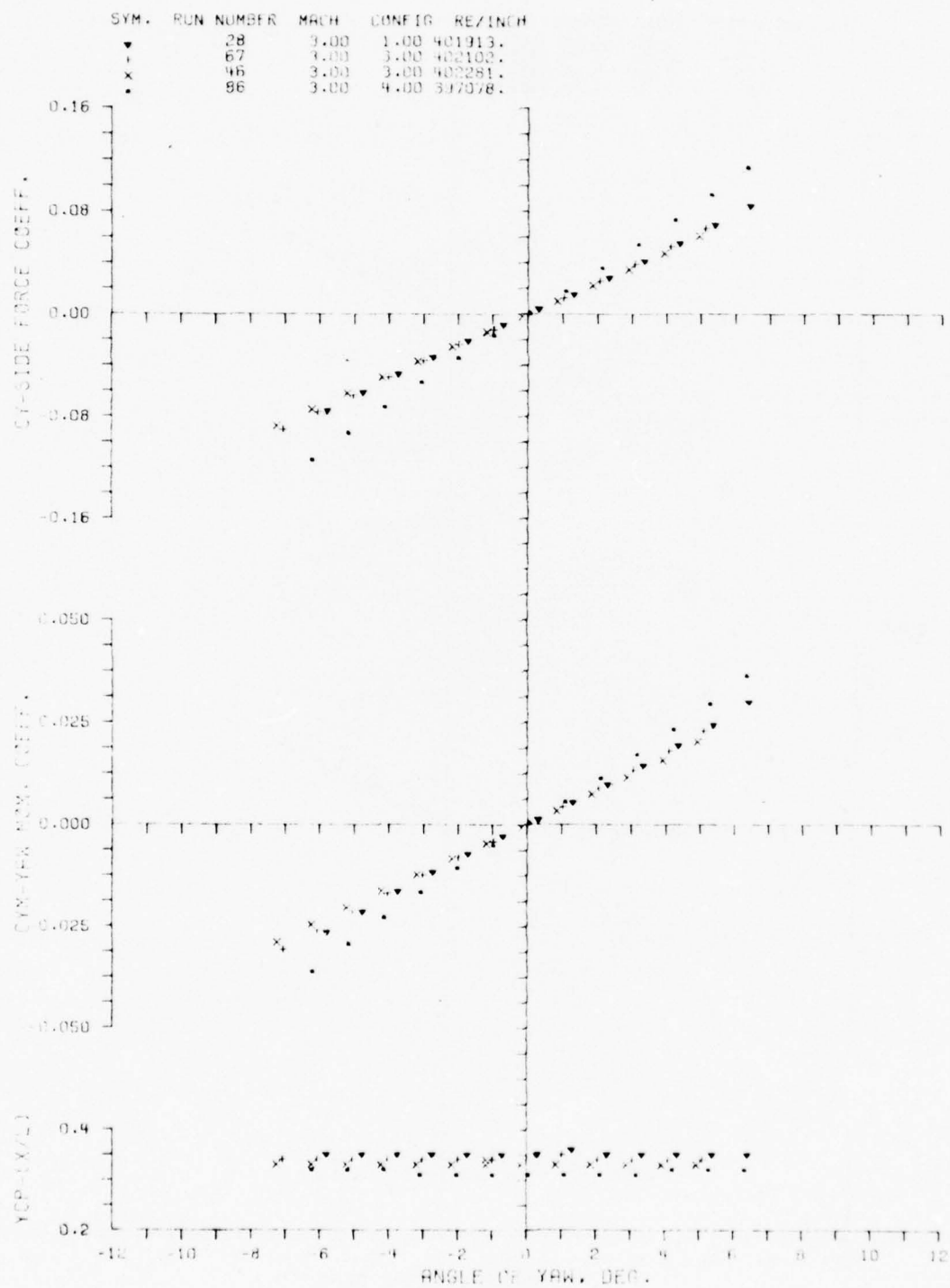
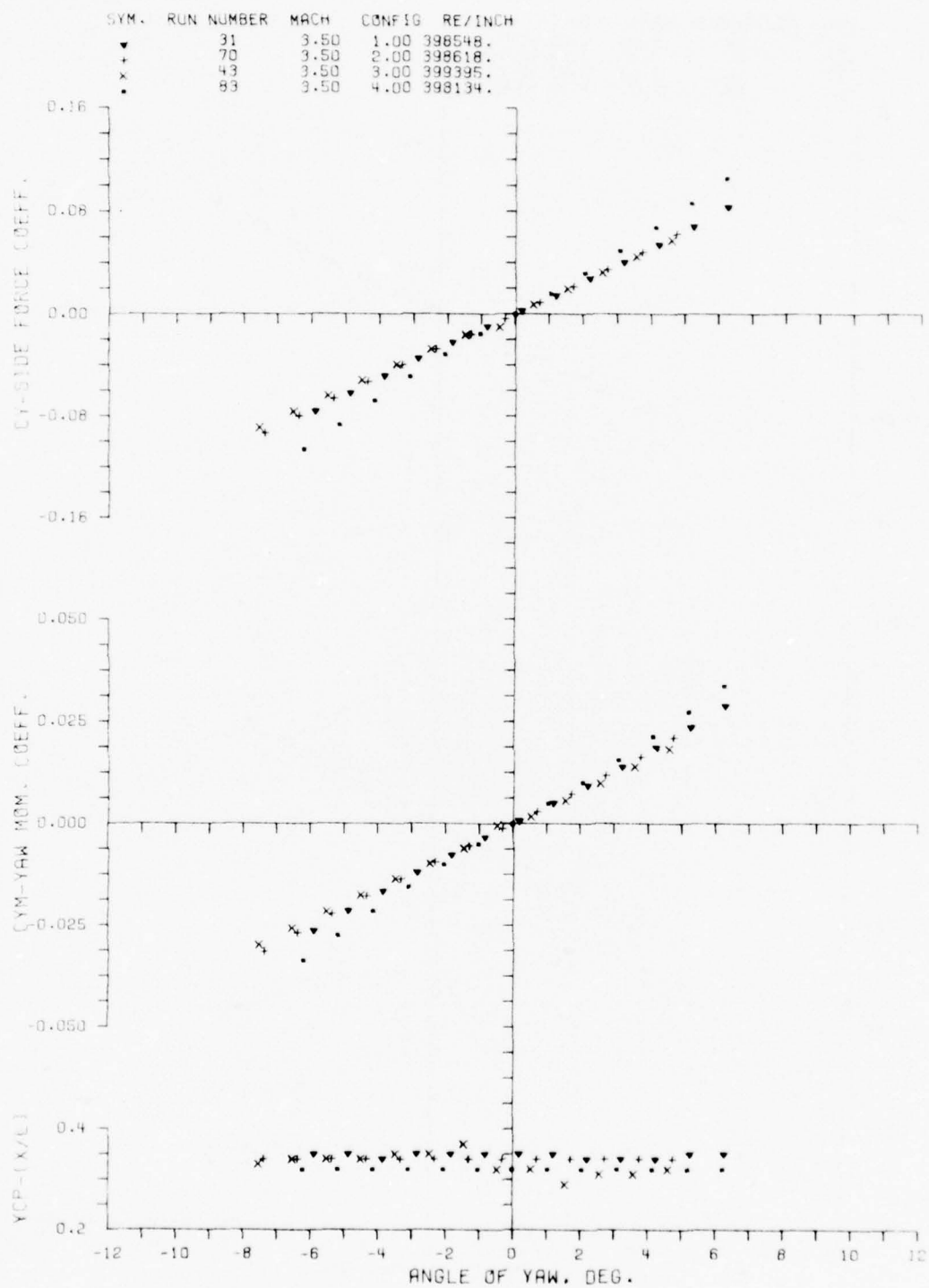


Figure A4. Continued

d. MACH 3.0



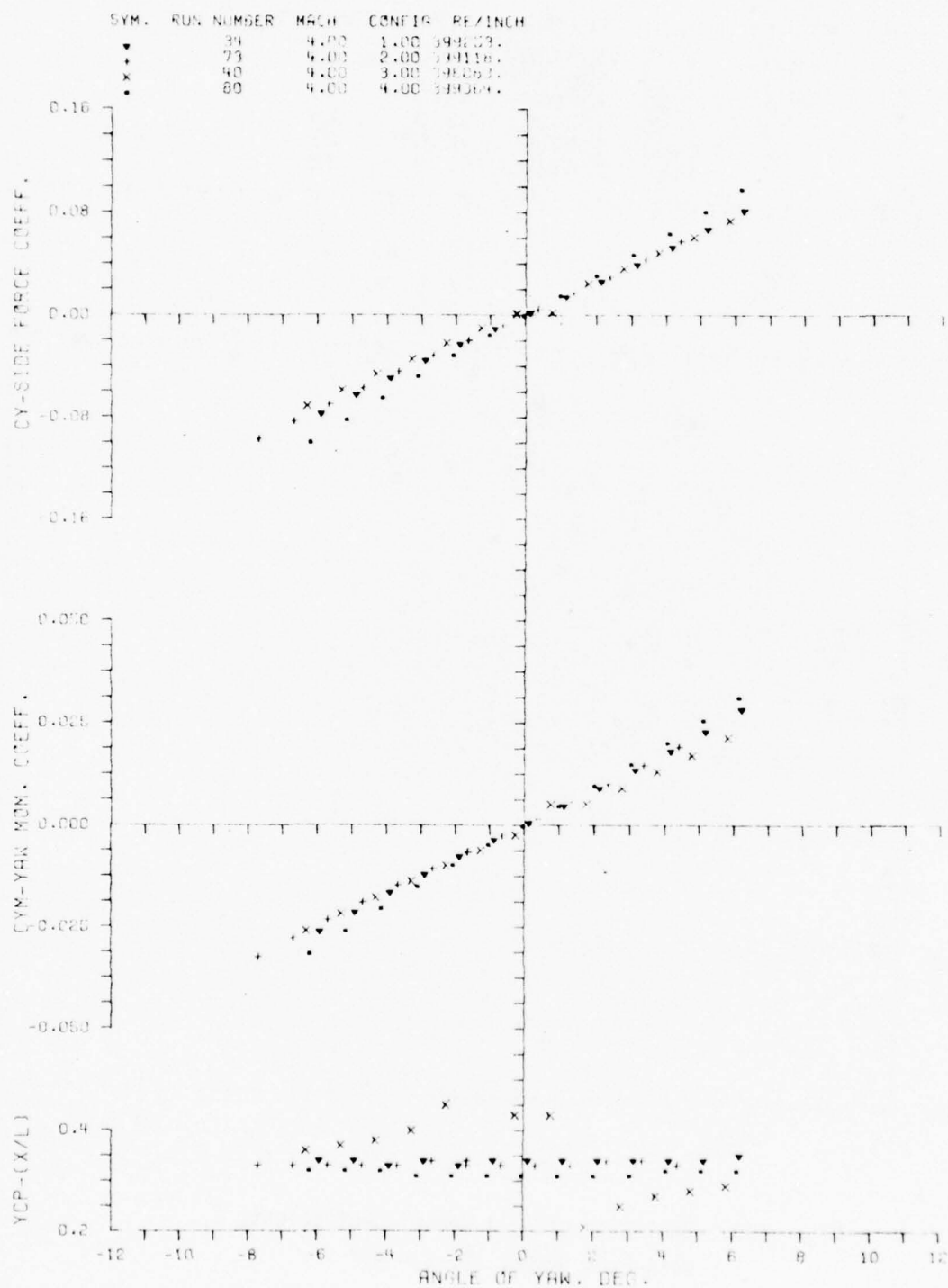


Figure A4. Concluded

f. MACH 4.0

SYM.	CONFIG	MACH	RE/INCH	PHI	RUN NO.
□	1.00	4.00	399728.	45.0	33
▲	1.00	3.50	398533.	45.0	30
▼	1.00	3.00	402095.	45.0	27
+	1.00	2.50	400795.	45.0	24
x	1.00	2.00	399746.	45.0	21
•	1.00	1.50	386312.	45.0	18

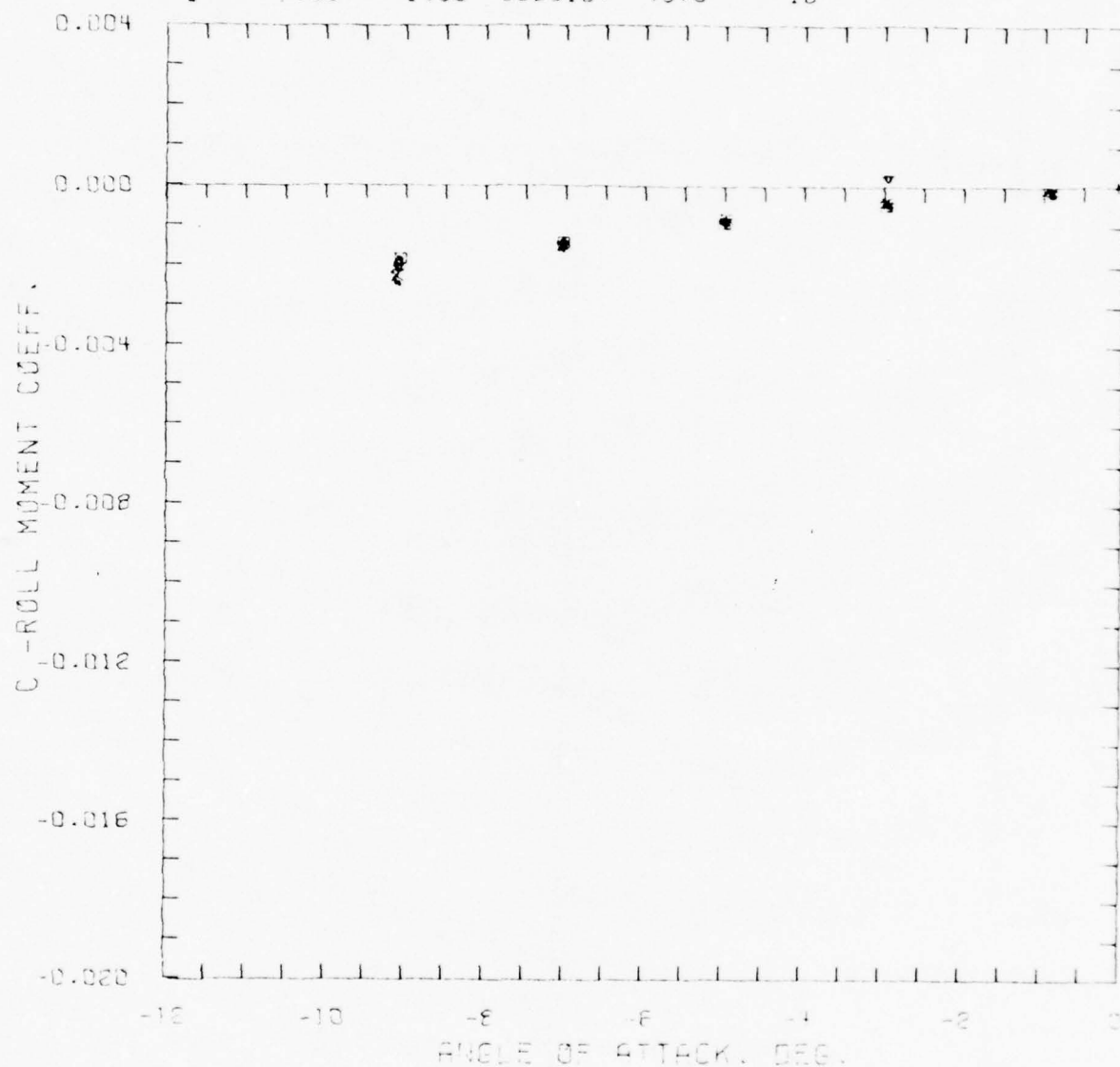


Figure A5. Variation of Roll Moment Coefficient, C_l ,
With Mach Number for $\phi = 45^\circ$

a. CONFIG 1.00

SYM.	CONFIG	MACH	RE/INCH	PHI	RUN NO.
□	2.00	4.00	398962.	45.0	72
▲	2.00	3.50	398013.	45.0	69
△	2.00	3.00	402240.	45.0	66
+	2.00	2.50	403610.	45.0	63
x	2.00	2.00	399250.	45.0	60
.	2.00	1.50	386835.	45.0	57

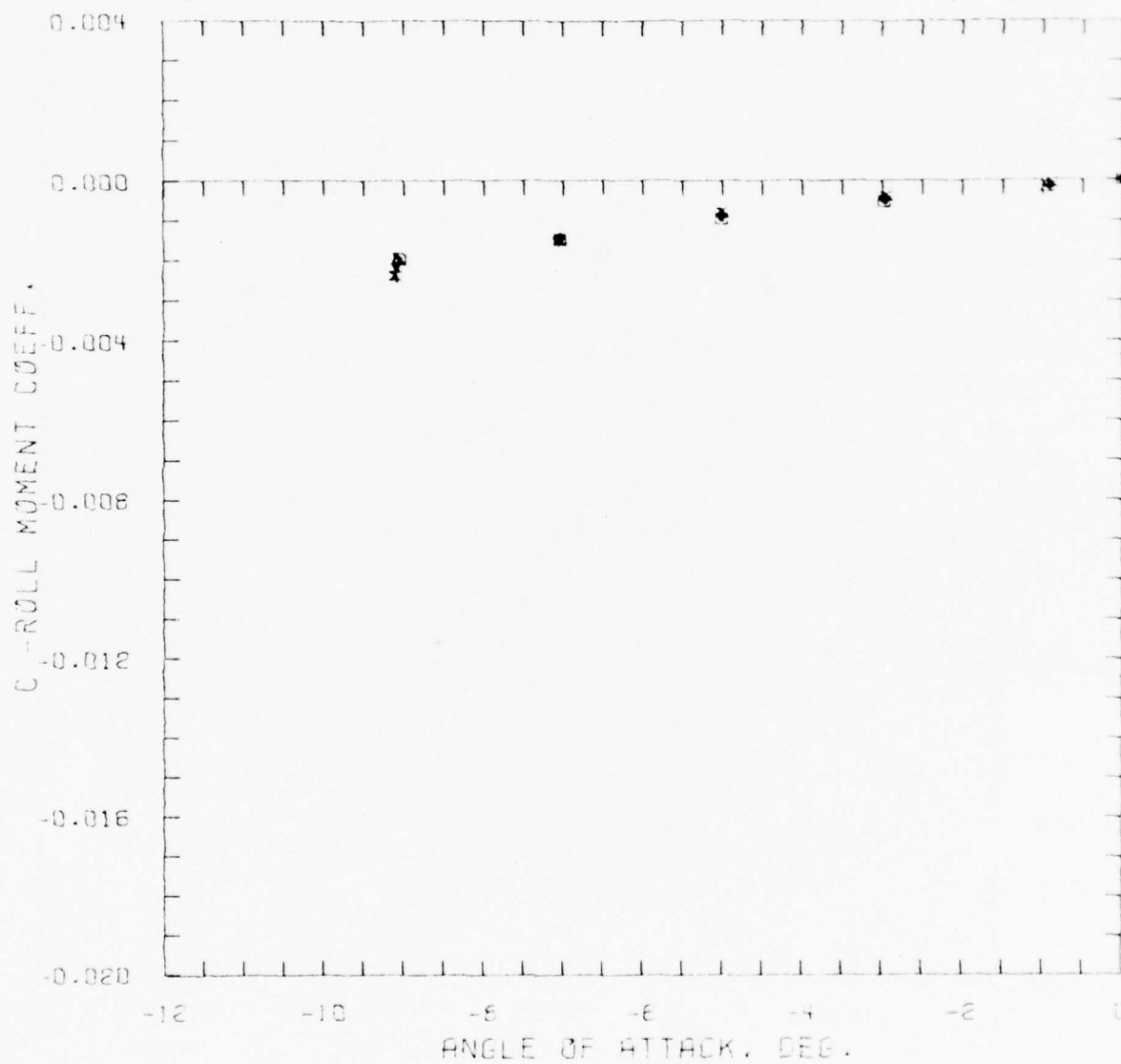


Figure A5. Continued

b. CONFIG 2.00

SYM.	CONFIG	MACH	RE/INCH	PHI	RUN NO.
□	3.00	4.00	398995.	45.0	39
▲	3.00	3.50	400493.	45.0	42
▼	3.00	3.00	403542.	45.0	45
+	3.00	2.50	399433.	45.0	48
x	3.00	2.00	399311.	45.0	51
.	3.00	1.50	386039.	45.0	54

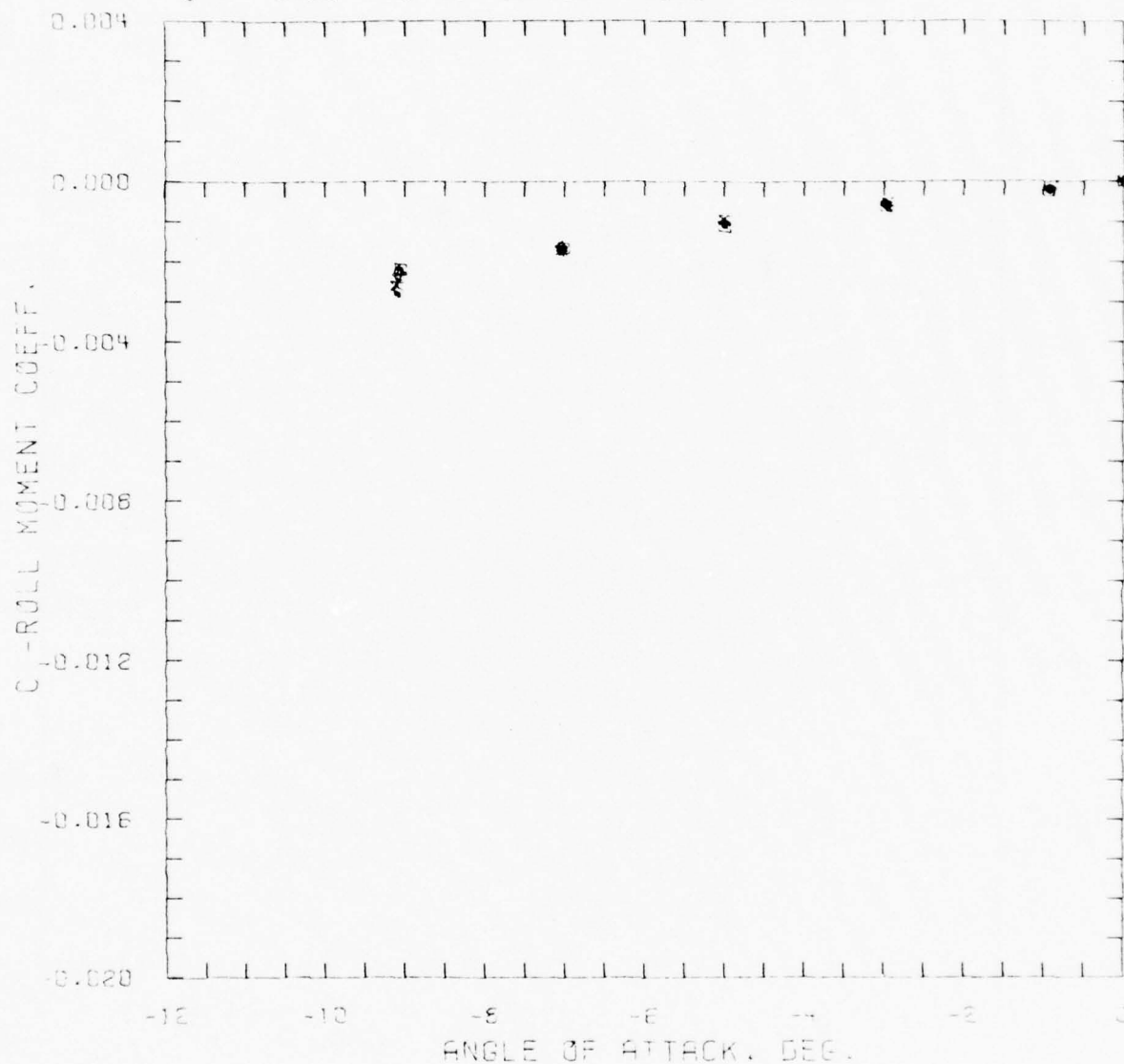


Figure A5. Continued

c. CONFIG 3.00

SYM.	CONFIG	MACH	RE/INCH	PHI	RUN NO.
□	4.00	4.00	398284.	45.0	79
▲	4.00	3.50	398184.	45.0	82
▼	4.00	3.00	403360.	45.0	85
+	4.00	2.50	395409.	45.0	88
x	4.00	2.00	398203.	45.0	91
.	4.00	1.50	385945.	45.0	94

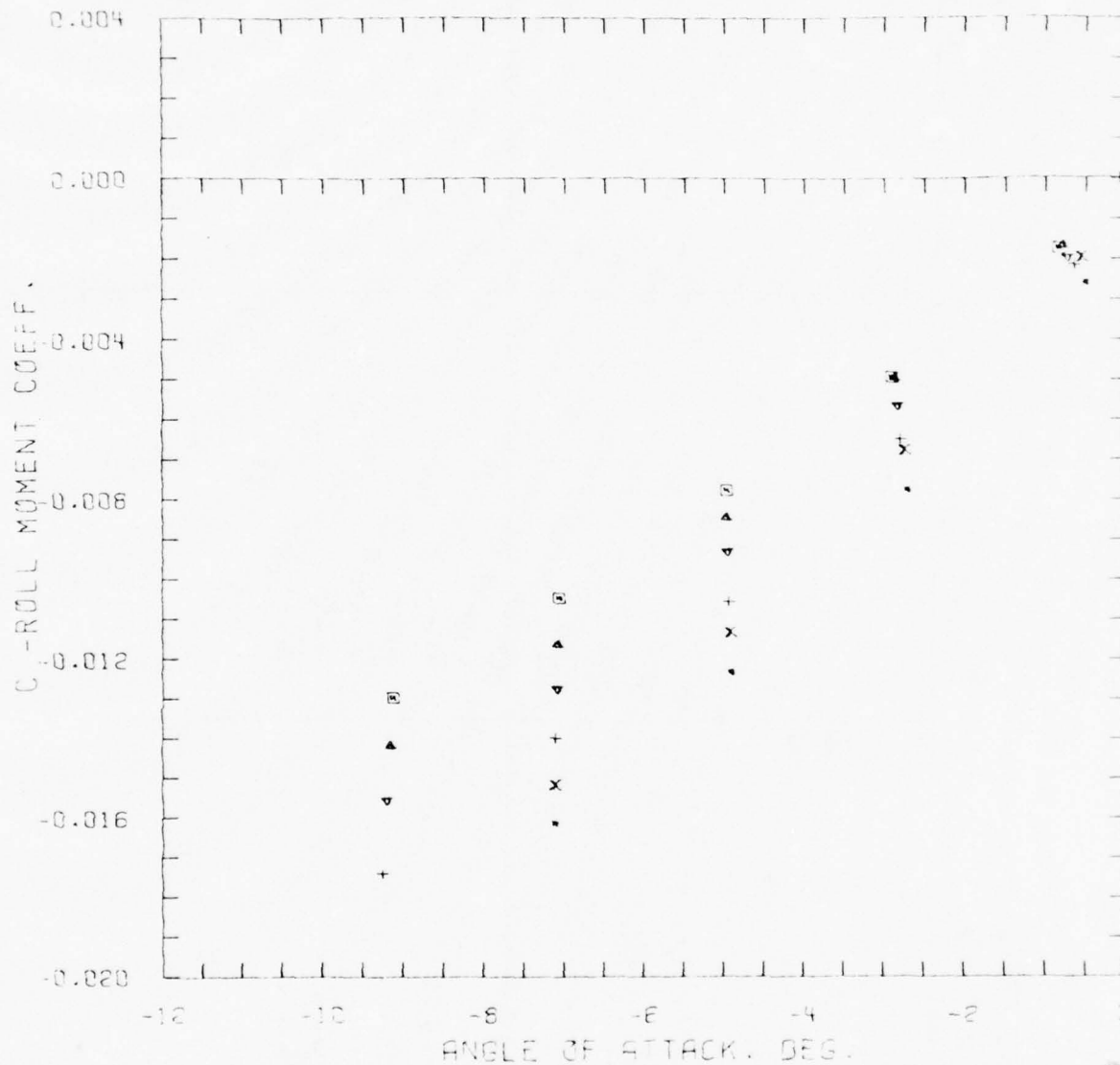


Figure A5. Concluded

d. CONFIG 4.00

BEST AVAILABLE COPY

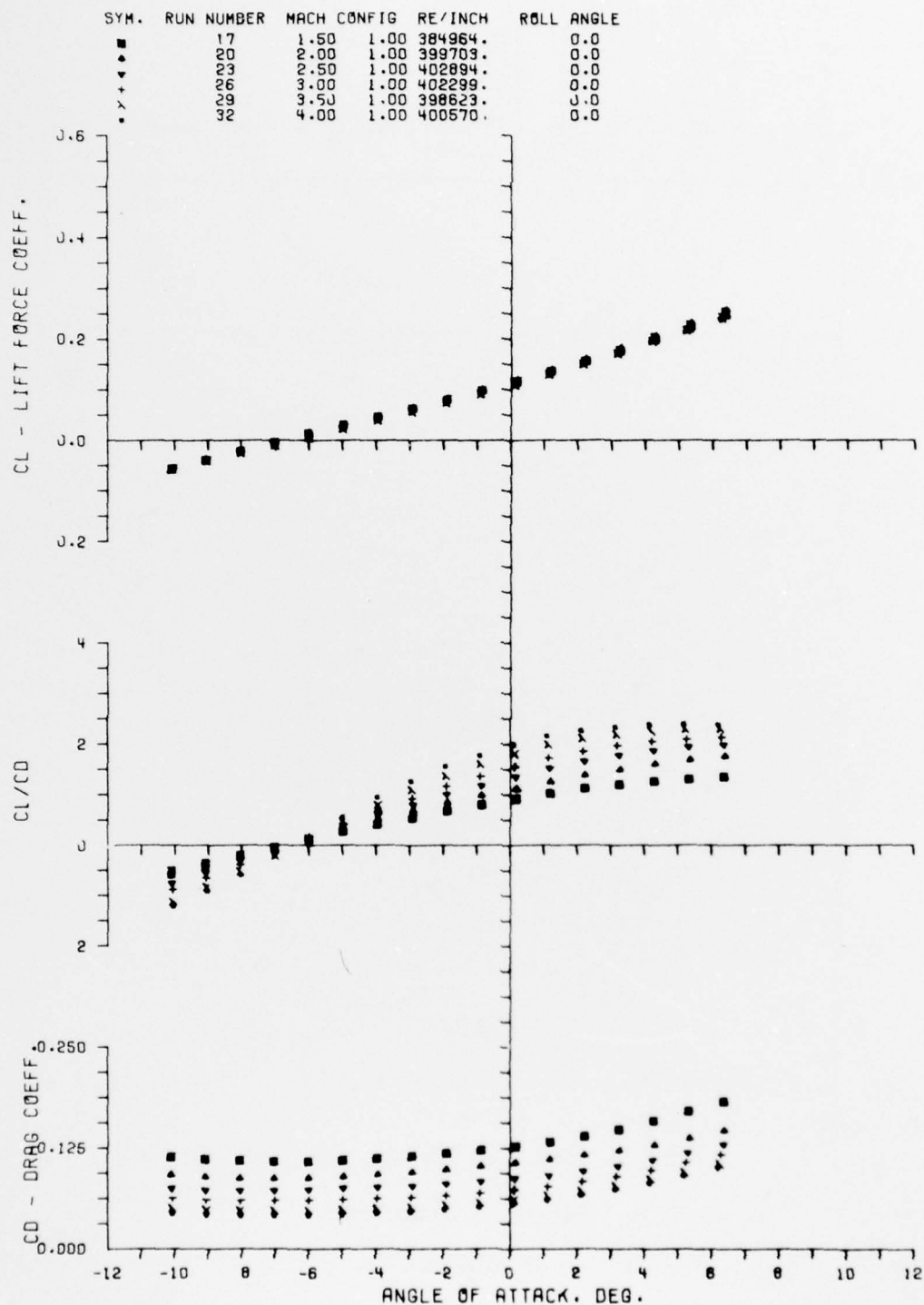


Figure A6. Aerodynamic Coefficients C_L , C_D , C_L/C_D --
Mach Number Variation

a. CONFIG 1.00

SYM.	RUN NUMBER	MACH	CONF	RE INCH	ROLL ANGLE
■	56	1.50	2.00	386890.	0.0
▲	59	2.00	2.00	399415.	0.0
△	62	2.50	2.00	402910.	0.0
+	65	3.00	2.00	402094.	0.0
x	68	3.50	2.00	396086.	0.0
.	71	4.00	2.00	399350.	0.0

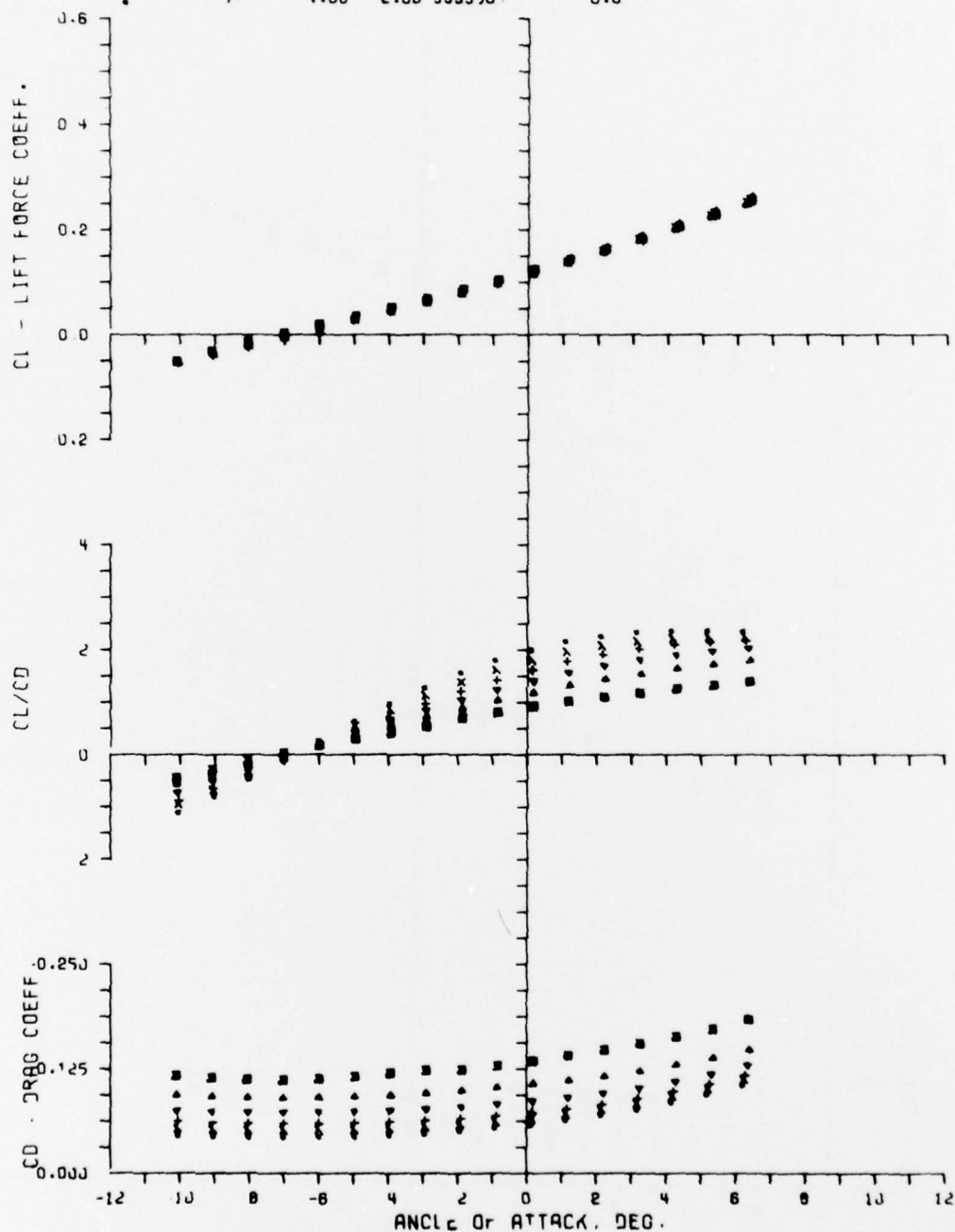


Figure A6. Continued

b. CONFIG 2.00

SYM.	RUN NUMBER	MACH	CONF	IG	RE/INCH	ROLL	ANGLE
53	1.50	3.00	385808.		0.0		
50	2.00	3.00	400082.		0.0		
47	2.50	3.00	400836.		0.0		
44	3.00	3.00	403510.		0.0		
41	3.50	3.00	398461.		0.0		
38	4.00	3.00	400383.		0.0		

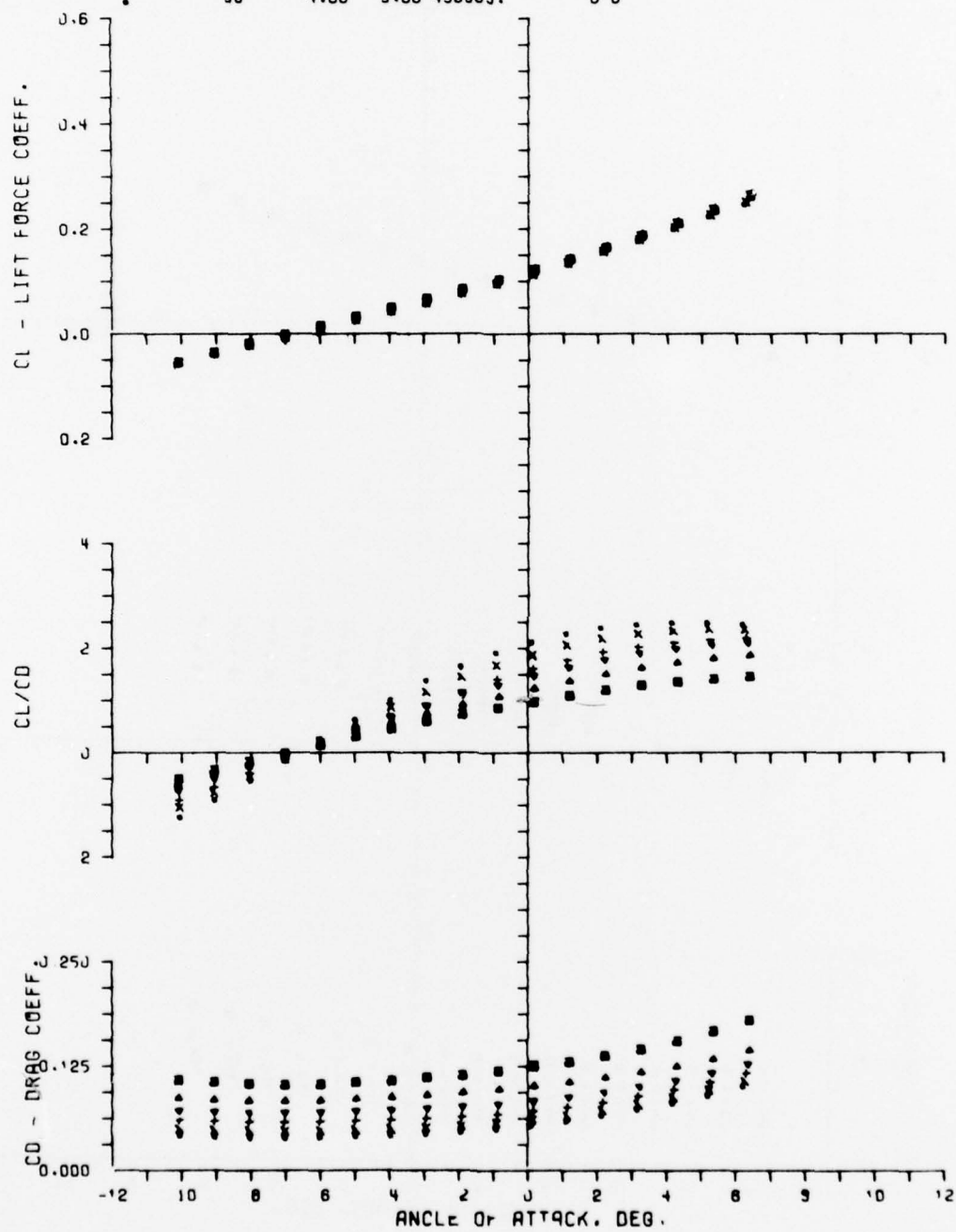


Figure A6. Continued

c. CONFIG 3.00

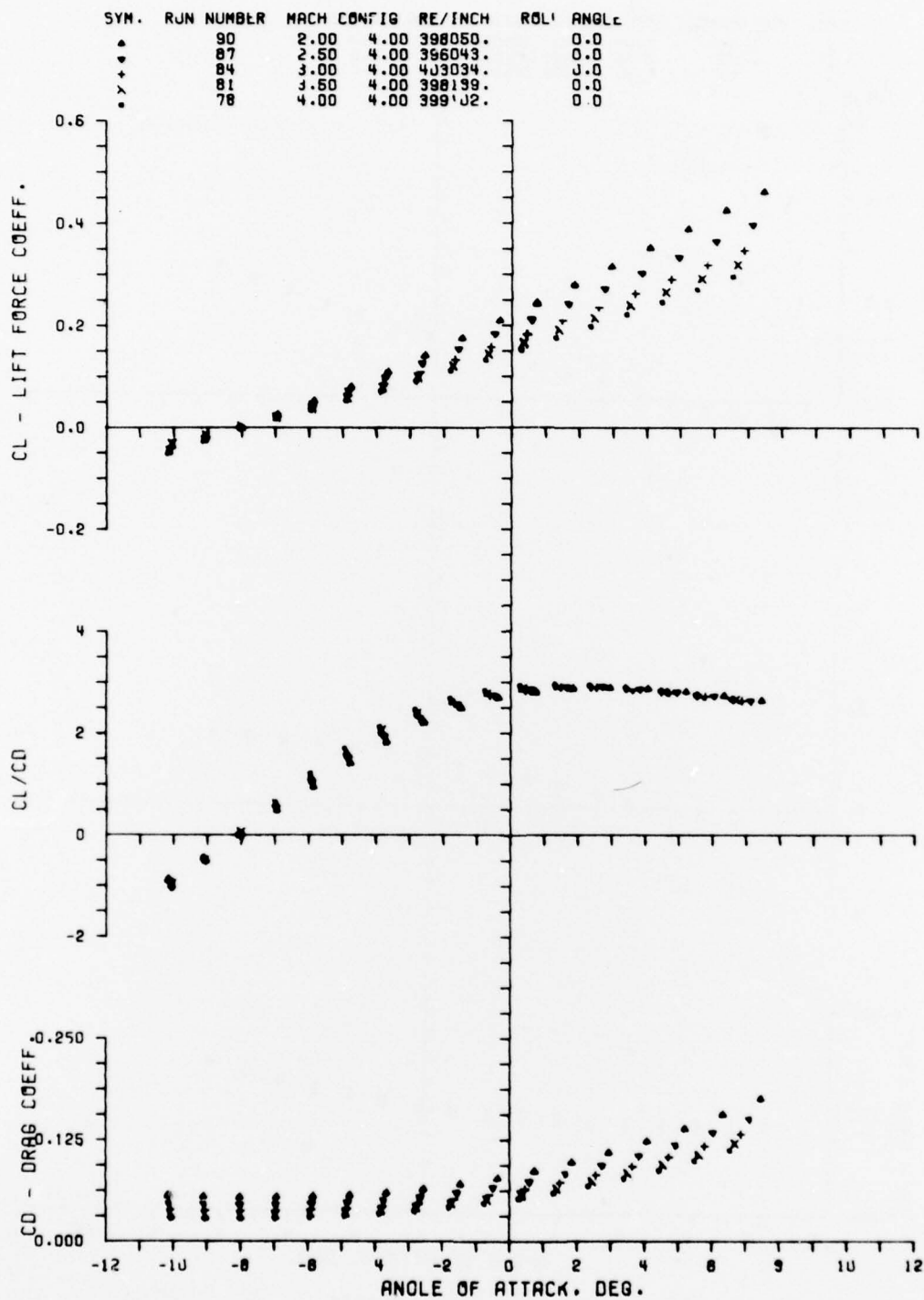


Figure A6. Concluded

d. CONFIG 4.00

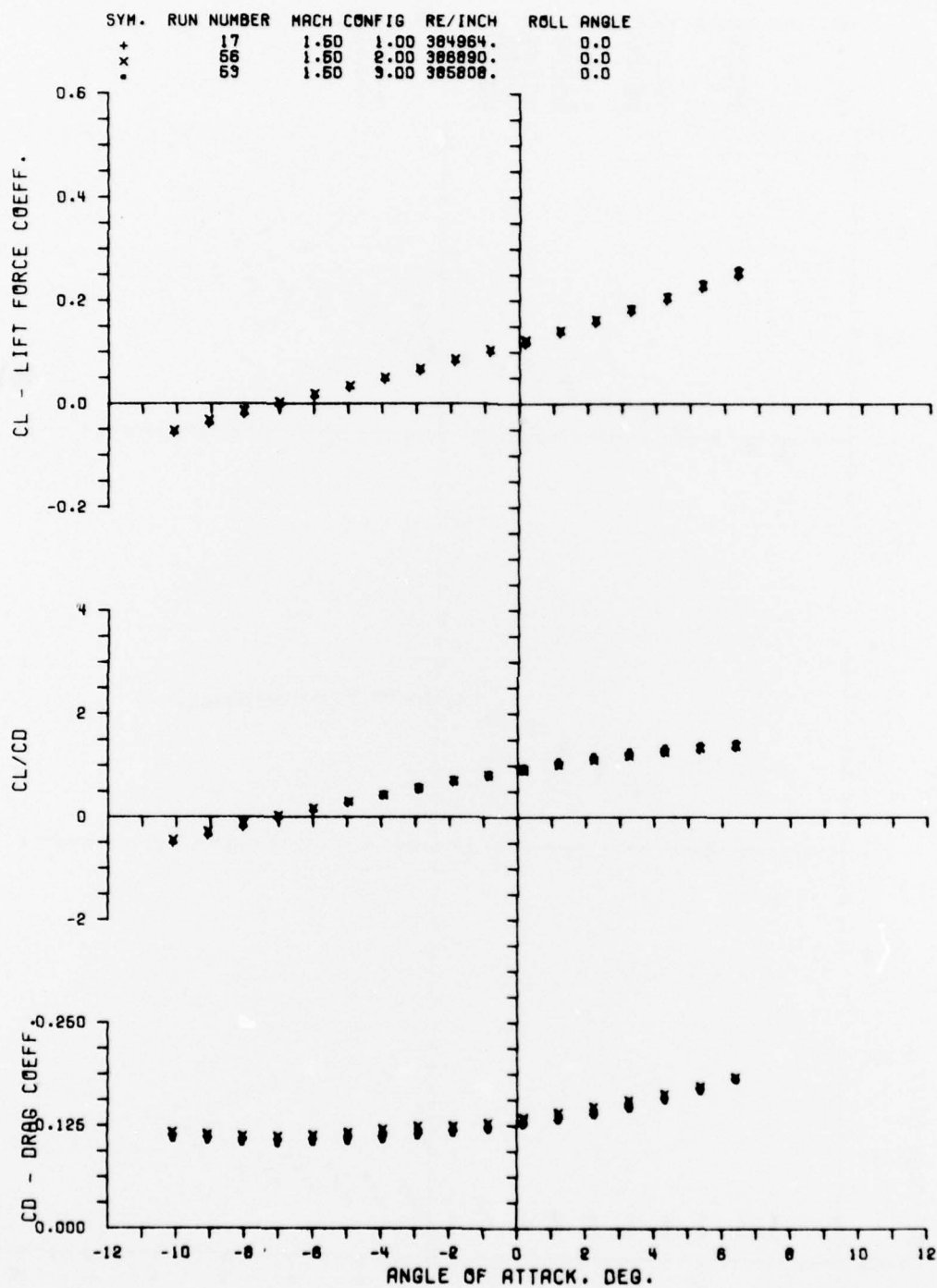


Figure A7. Aerodynamic Coefficients C_L , C_D , C_L/C_D --
Configuration Variation

a. MACH 1.5

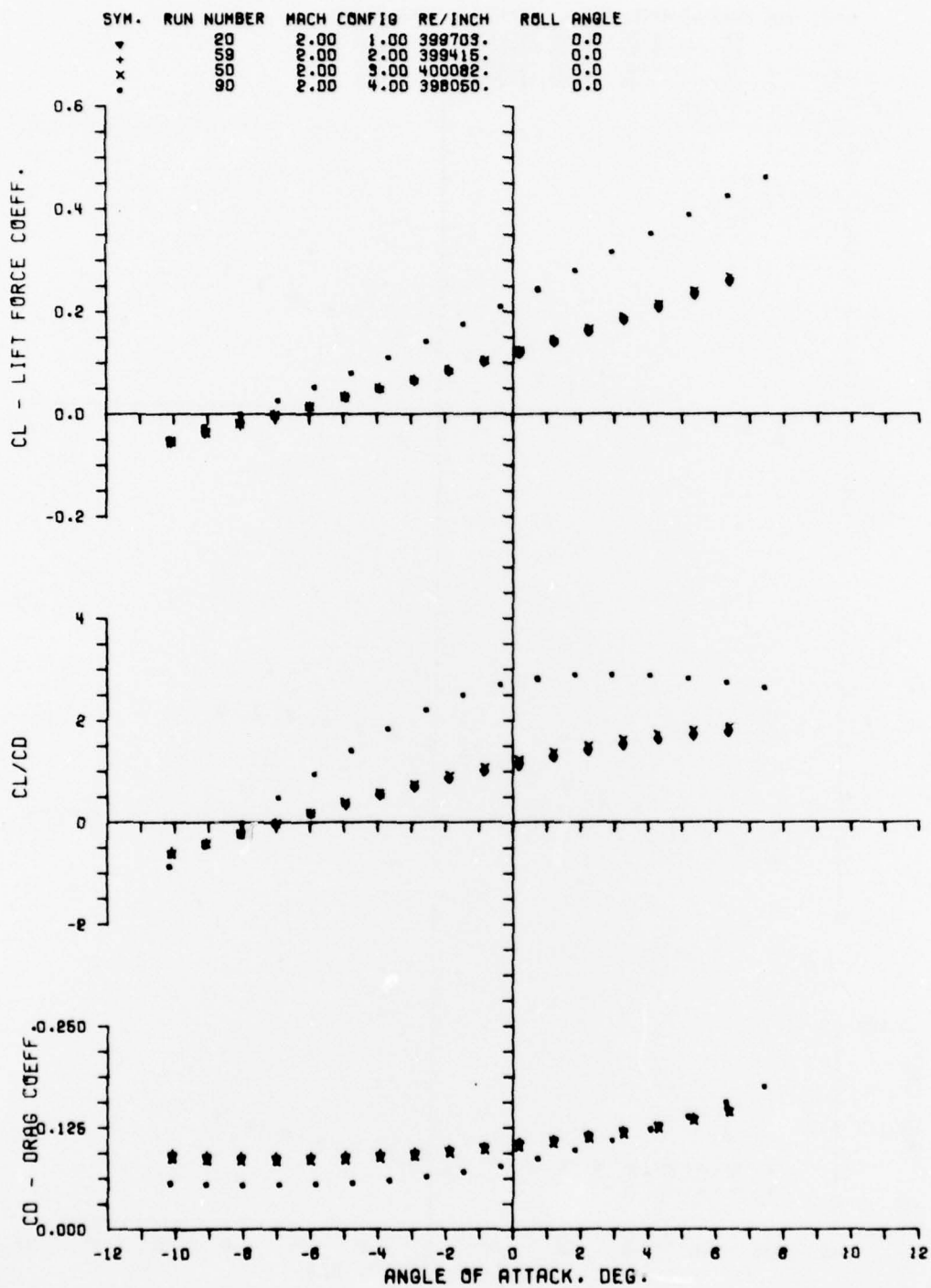


Figure A7. Continued

b. MACH 2.0

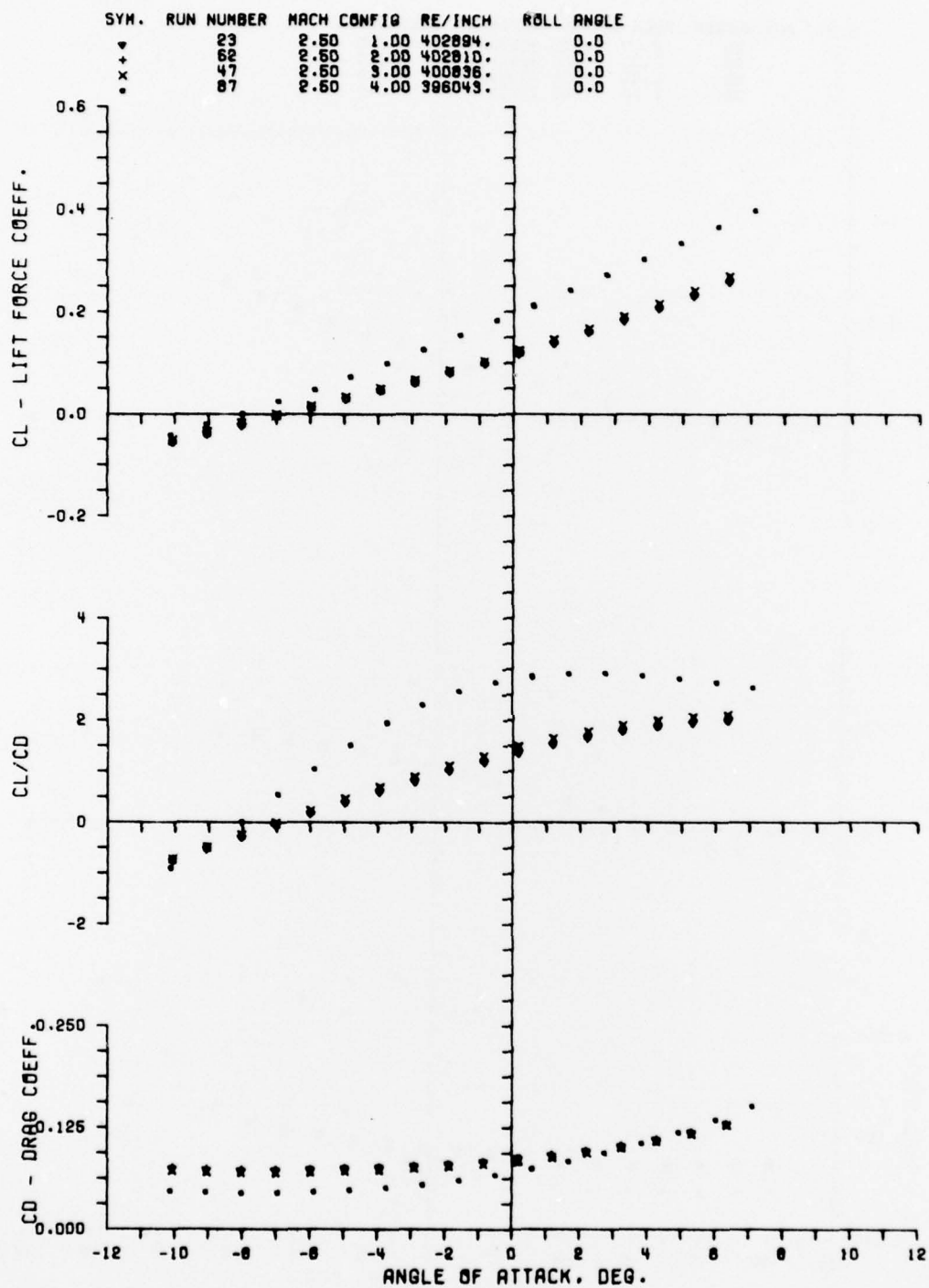


Figure A7. Continued

c. MACH 2.5

SYM.	RUN NUMBER	MACH	CONFIG	RE/INCH	ROLL ANGLE
+	26	3.00	1.00	402299.	0.0
x	66	3.00	2.00	402094.	0.0
.	44	3.00	3.00	403510.	0.0
.	84	3.00	4.00	403034.	0.0

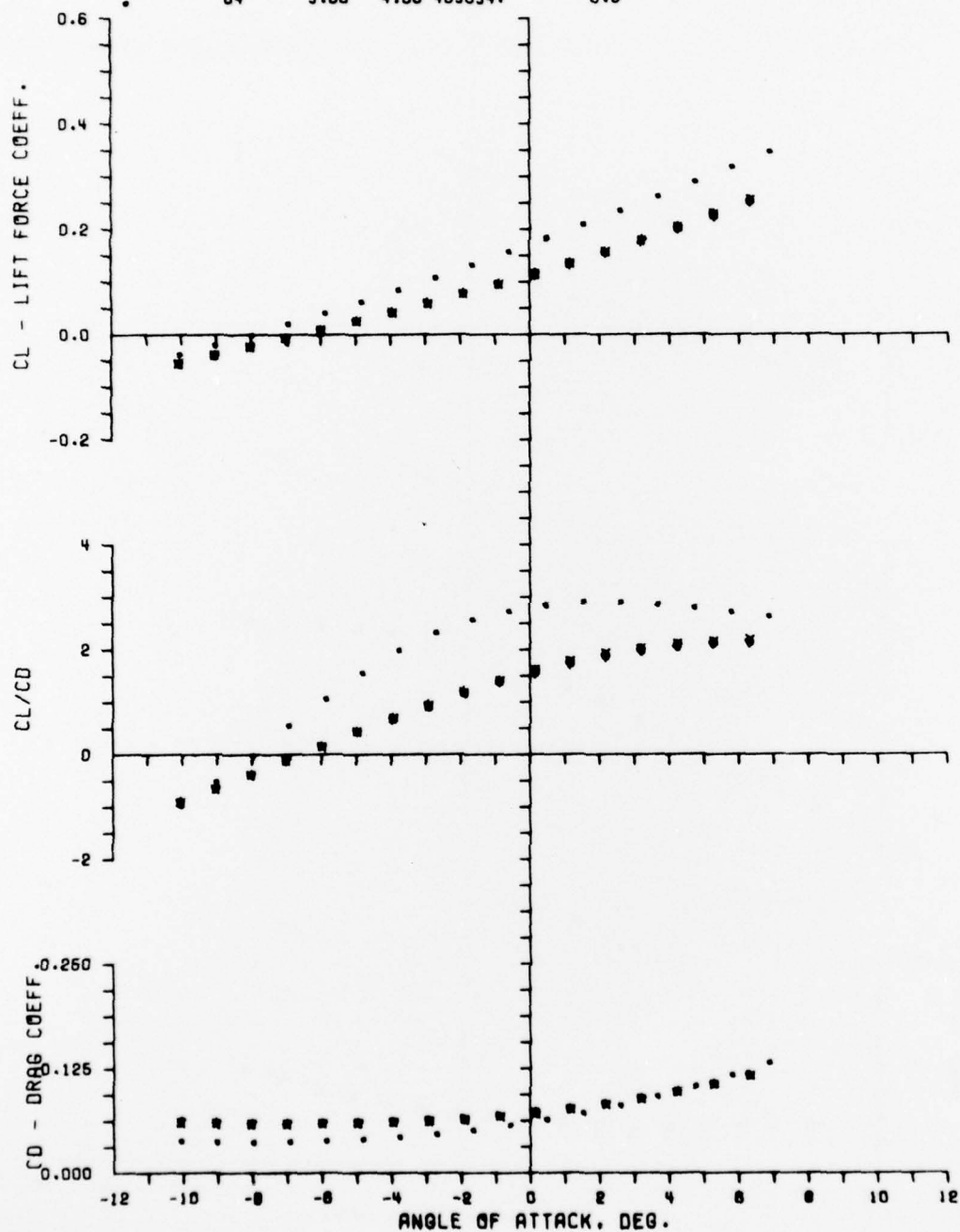


Figure A7. Continued

d. MACH 3.0

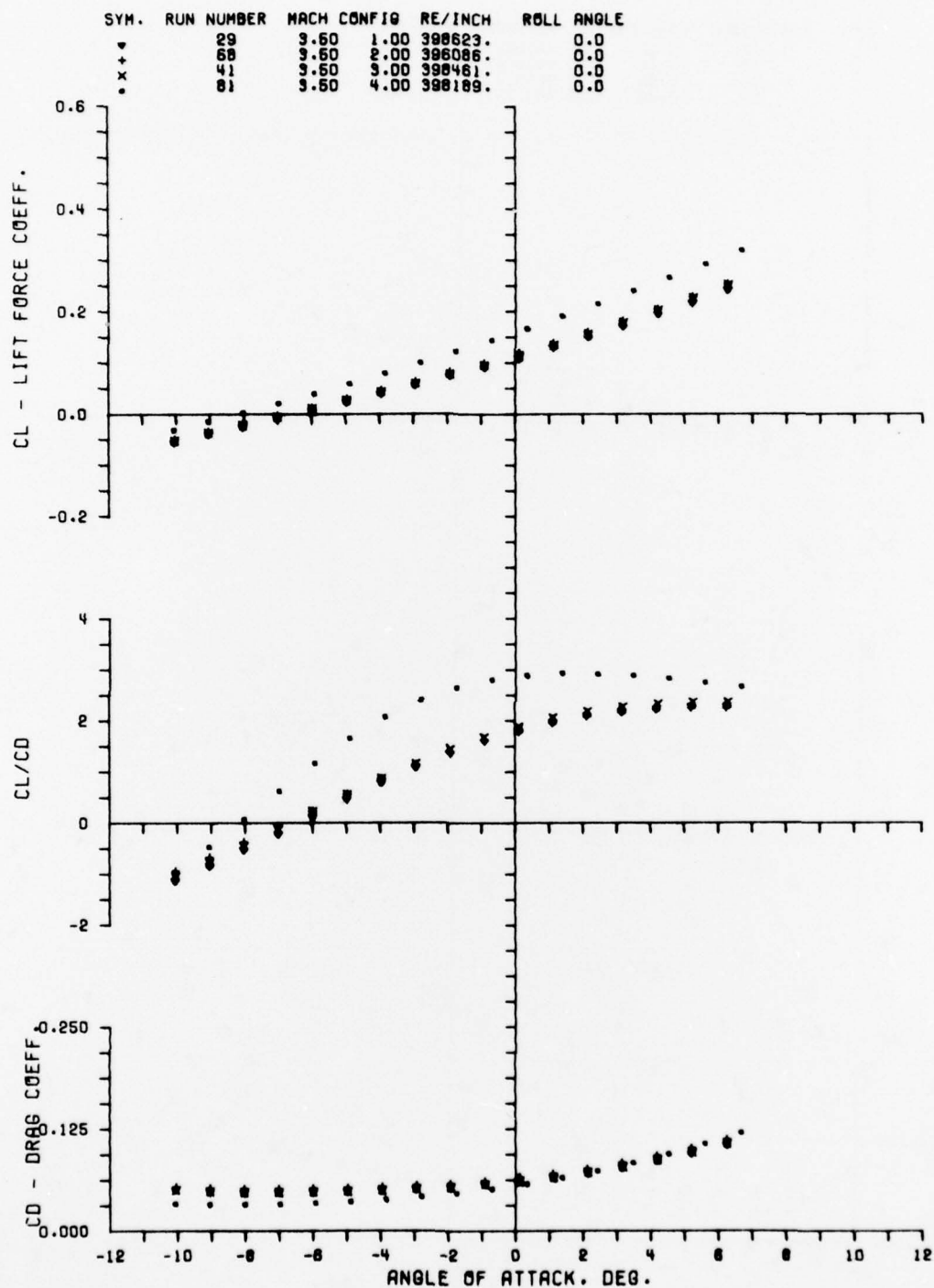


Figure A7. Continued

e. MACH 3.5

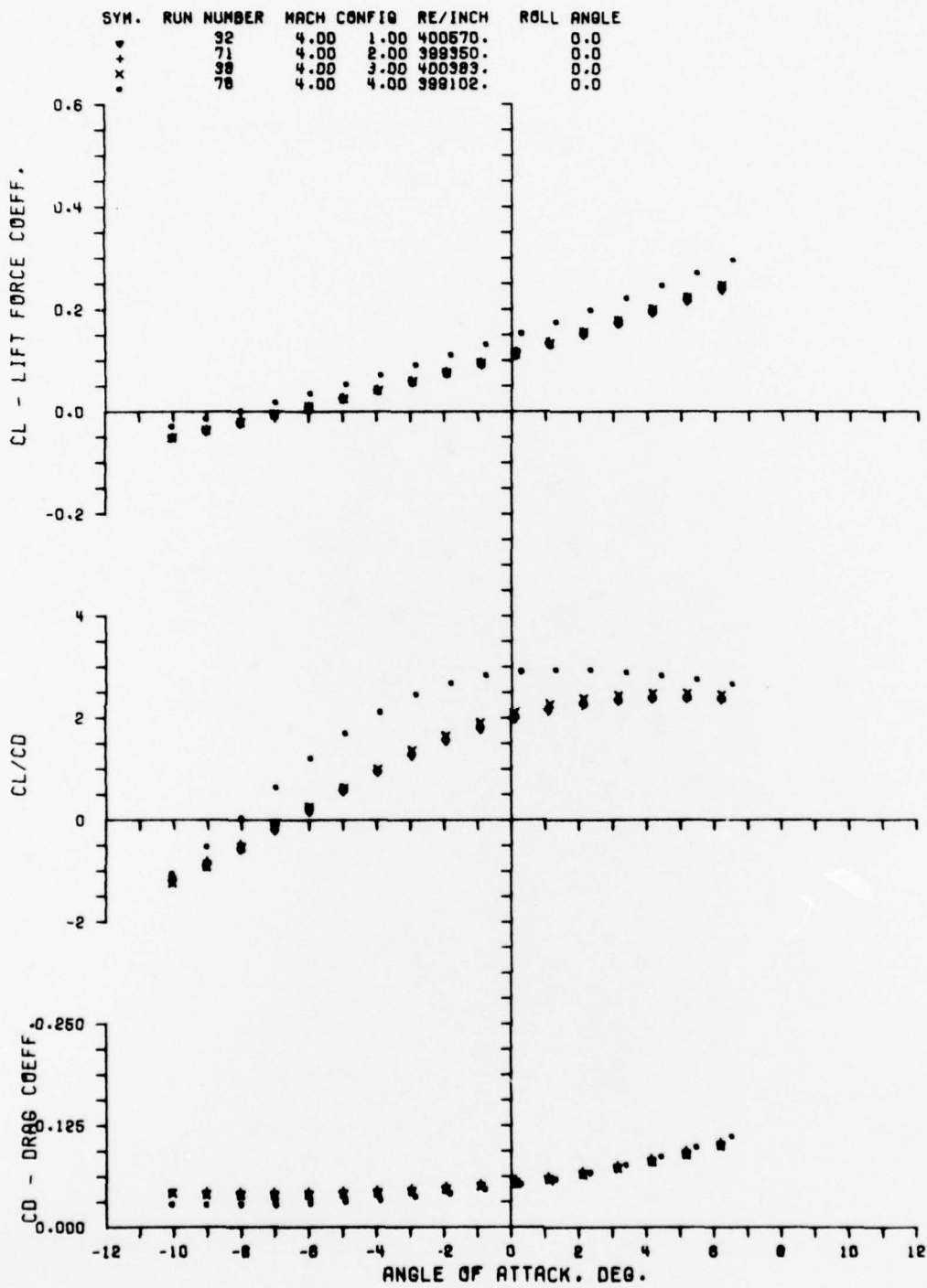


Figure A7. Concluded

f. MACH 4.0

LIST OF SYMBOLS

b	model base width
C_A	axial-force coefficient, $F_A/(qS)$
C_D	drag-force coefficient, $F_D/(qS)$
C_L	lift-force coefficient, $F_L/(qS)$
C_{L_α}	lift-force coefficient slope about trim angle
C_m	pitching-moment coefficient, $m/(qS\ell)$, reference at the model base
C_n	yawing-moment coefficient, $n/(qS\ell)$, reference at the model base
C_N	normal-force coefficient, $F_N/(qS)$
C_Y	side-force coefficient, $F_Y/(qS)$
F_A	axial-force
F_D	drag-force, $F_A \cos \alpha + F_N \sin \alpha$
F_L	lift-force, $F_N \cos \alpha - F_A \sin \alpha$
F_N	normal force
F_Y	side force
ℓ	model length
m	pitching moment
M	Mach number
n	yawing moment
q	free-stream dynamic pressure
Re	Reynolds number, based on free-stream conditions

LIST OF SYMBOLS (Continued)

S	reference planform area, $1/2[b\ell]$
X_{CP}	location of normal-force center of pressure, normalized with respect to model length, ℓ , and referenced at the model base
Y_{CP}	location of side-force center of pressure, normalized with respect to model length, ℓ , and referenced at the model base
α	angle of attack
ψ	angle of yaw

DISTRIBUTION LIST

<u>No. of</u> <u>Copies</u>	<u>Organization</u>	<u>No. of</u> <u>Copies</u>	<u>Organization</u>
12	Commander Defense Documentation Center ATTN: DDC-TCA Cameron Station Alexandria, VA 22333	1	Commander US Army Tank Automotive Development Command ATTN: DRDTA-RWL Warren, MI 48090
1	Commander US Army Materiel Development and Readiness Command ATTN: DRCDMA-ST 5001 Eisenhower Avenue Alexandria, VA 22333	2	Commander US Army Mobility Equipment Research & Development Command ATTN: Tech Docu Cen, Bldg. 315 DRSME-RZT Fort Belvoir, VA 22060
1	Commander US Army Aviation Systems Command ATTN: DRSAB-E 12th and Spruce Streets St. Louis, MO 63166	1	Commander US Army Armament Command Rock Island, IL 61202
1	Director US Army Air Mobility Research and Development Laboratory Ames Research Center Moffett Field, CA 94035	2	Commander US Army Frankford Arsenal ATTN: Mr. Spencer Hirschman Mr. John Sikra Bridge and Tacony Streets Philadelphia, PA 19137
1	Commander US Army Electronics Command ATTN: DRSEL-RD Fort Monmouth, NJ 07703	4	Commander US Army Picatinny Arsenal ATTN: SARPA-AD Mr. S. Wasserman SARPA-FR-S-A Mr. D. Mertz Mr. E. Falkowski Mr. A. Loeb Dover, NJ 07801
1	Commander US Army Jefferson Proving Ground ATTN: STEJP-TD-D Madison, IN 47250	1	Commander US Army Harry Diamond Labs ATTN: DRXDO-TI 2800 Powder Mill Road Adelphi, MD 20783
3	Commander US Army Missile Command ATTN: DRSMI-R DRSMI-RDK Mr. R. Deep Mr. R. Becht Redstone Arsenal, AL 35809	1	Commander US Army Natick Research and Development Command ATTN: DRXRE, Dr. D. Sieling Natick, MA 01762

DISTRIBUTION LIST

<u>No. of</u> <u>Copies</u>	<u>Organization</u>	<u>No. of</u> <u>Copies</u>	<u>Organization</u>
1	Director US Army TRADOC Systems Analysis Activity ATTN: ATAA-SA White Sands Missile Range NM 88002	1	Director Jet Propulsion Laboratory ATTN: Mr. B. Dayman 4800 Oak Grove Drive Pasadena, CA 91103
1	Commander US Army Research Office P. O. Box 12211 Research Triangle Park NC 27709	1	Calspan Corporation ATTN: Mr. J. Andes, Head Transonic Tunnel Dept P. O. Box 235 Buffalo, NY 14221
3	Commander US Naval Air Systems Command ATTN: AIR-604 Washington, DC 20360	1	Honeywell, Inc. ATTN: Mr. George Stilley 600 Second Street, N Hopkins, MN 55343
2	Commander David W. Taylor Naval Ship Research and Development Ctr ATTN: Dr. S. de los Santos Mr. Stanley Gottlieb Bethesda, MD 20084	1	Sandia Laboratories ATTN: Division No. 9322 Mr. Warren Curry P. O. Box 5800 Albuquerque, NM 87115
1	Commander US Naval Surface Weapons Center ATTN: Dr. T. Clare, Code DK20 Dahlgren, VA 22448	2	Massachusetts Institute of Technology ATTN: Prof. E. Covert Prof. C. Haldeman 77 Massachusetts Avenue Cambridge, MA 02139
2	Commander US Naval Surface Weapons Center ATTN: Code 312, S. Hastings Mr. F. Regan Silver Spring, MD 20910	2	MIT/Lincoln Laboratories ATTN: Dr. Milan Vlainac Mr. Charles Bruce Mail Stop D-382 P. O. Box 73 Lexington, MA 02173
1	Commander US Naval Weapons Center ATTN: Code 5115 Dr. A. Charters China Lake, CA 93555	1	Rutgers University Mechanical, Industrial, and Aerospace Engineering Dept ATTN: Dr. Robert H. Page New Brunswick, NJ 08903
1	AFATL (DLDL) Eglin AFB, FL 32542		

DISTRIBUTION LIST

<u>No. of Copies</u>	<u>Organization</u>
1	University of Virginia Department of Aerospace Engineering and Engineering Physics ATTN: Prof. I. Jacobson Charlottesville, VA 22904

Aberdeen Proving Ground

Marine Corps Ln Ofc
Dir, USAMSAA
Cdr, USAEA
ATTN: SAREA-DE-W
Mr. A. Flatau
Mr. J. Huerta